

# In situ metabolomic analysis of Setaria viridis roots colonized by beneficial endophytic bacteria

Journal:	Molecular Plant-Microbe Interactions
Manuscript ID	MPMI-06-19-0170-R
Manuscript Type:	Research
Date Submitted by the Author:	27-Jun-2019
Complete List of Authors:	Agtuca, Beverly; University of Missouri Columbia, Plant Sciences Stopka, Sylwia; George Washington University TULESKI, THALITA; Universidade Federal do Parana, Biochemistry and Molecular Biology Amaral, Fernanda; University of Missouri, Divisions of Plant Science and Biochemistry Evans, Sterling; University of Missouri Columbia, Plant Sciences Liu, Yang; University of Missouri Columbia Xu, Dong; Univ. of Missouri, Computer Science Adele Monteiro, Rose; Universidade Federal do Parana, Biochemistry and Molecular Biology Koppenaal, David; Pacific Northwest National Laboratory Paša-Tolić, Ljiljana; Pacific Northwest National Laboratory Anderton, Christopher; Pacific Northwest National Laboratory Vertes, Akos; George Washington University Stacey, Gary; University of Missouri, Department of Plant Microbiology and Pathology
Area That Best Describes Your Manuscript:	Bacteria-plant symbiosis, non-Rhizobium nitrogen fixation < Bacteria- plant symbiosis, Endophytes, Secondary metabolism, Biocontrol

SCHOLARONE™ Manuscripts

	Agtuca MPMI
1	In situ metabolomic analysis of Setaria viridis roots colonized
2	by beneficial endophytic bacteria
3	AUTHORS
4	Beverly J. Agtuca, <sup>1</sup> Sylwia A. Stopka, <sup>2</sup> Thalita R. Tuleski, <sup>1,3</sup> Fernanda P. do Amaral, <sup>1</sup>
5	Sterling Evans, <sup>1</sup> Yang Liu, <sup>4</sup> Dong Xu, <sup>4</sup> Rose Adele Monteiro, <sup>3</sup> David W. Koppenaal, <sup>5</sup>
6	Ljiljana Paša-Tolić, <sup>5</sup> Christopher R. Anderton, <sup>5</sup> Akos Vertes, <sup>2</sup> and Gary Stacey <sup>1†</sup>
7	AFFILATIONS
8	<sup>1</sup> Divisions of Plant Sciences and Biochemistry, Christopher S. Bond Life Sciences
9	Center, University of Missouri, Columbia, MO 65211, USA
10	<sup>2</sup> Department of Chemistry, The George Washington University, Washington, DC 20052,
11	USA
12	<sup>3</sup> Department of Biochemistry and Molecular Biology, Federal University of Paraná, CP
13	19046, 81.531-990 Curitiba, PR, Brazil
14	<sup>3</sup> Department of Electrical Engineering and Computer Science, Informatics Institute and
15	Christopher S. Bond Life Sciences Center, University of Missouri-Columbia, MO 65211,
16	USA
17	<sup>4</sup> Environmental Molecular Sciences Laboratory, Earth and Biological Sciences
18	Directorate, Pacific Northwest National Laboratory, 902 Battelle Boulevard, Richland,
19	Washington 99354, USA
20	

Agtuca MPMI

# 22 †Author for correspondence:

- Tel: +01 5738844752; E-mail: staceyg@missouri.edu
- 24 Dr. Gary Stacey
- 25 Curators' Distinguished Professor
- 26 Divisions of Plant Sciences and Biochemistry
- 27 271E Christopher S. Bond Life Sciences Center
- University of Missouri, Columbia, MO 65211

# ABSTRACT (235/250 WORDS)

Over the past decades, crop yields have risen in parallel with increasing use of fossil-fuel derived nitrogen (N) fertilizers, but with concomitant negative impacts on climate and water resources. There is a need for more sustainable agricultural practices, and biological nitrogen fixation (BNF) could be part of the solution. A variety of nitrogen-fixing, epiphytic and endophytic plant growth promoting bacteria (PGPB) are known to stimulate plant growth. However, compared to the rhizobium-legume symbiosis, little mechanistic information is available as to how PGPB affect plant metabolism. Therefore, we investigated the metabolic changes in roots of the model grass species *Setaria viridis* upon endophytic colonization by *Herbaspirillum seropedicae* SmR1 (fix+) or a fix mutant strain (SmR54), compared to uninoculated roots. Endophytic colonization of the root is highly localized and, hence, analysis of whole root segments dilutes the metabolic signature of those few cells impacted by the bacteria. Therefore, we utilized *in situ* laser ablation electrospray ionization mass spectrometry (LAESI-MS) to sample only those root segments at or adjacent to the sites of bacterial colonization. Metabolites involved in

MPMI

purine, zeatin, and riboflavin pathways were significantly more abundant in inoculated plants while metabolites indicative of nitrogen, starch, and sucrose metabolism were reduced in roots inoculated with the fix- strain or uninoculated, presumably due to N limitation. Interestingly, compounds, involved in indole-alkaloid biosynthesis were more abundant in the roots colonized by the fix- strain, perhaps reflecting a plant defense response.

#### **KEYWORDS**

**Agtuca** 

Nitrogen fixation, metabolites, *Herbaspirillum seropedicae*, PGPB, associative bacteria, plant growth promotion, *nifA*, rhizosphere, mass spectrometry, laser ablation electrospray ionization

## **INTRODUCTION**

Plant development and productivity rely on nutrients that are naturally available in the soil. However, in many situations, specific nutrients necessary for plant growth are present in low abundance or may not be available in a form that can be readily absorbed by the roots. For instance, nitrogen is a critical macronutrient for plant growth and is commonly a limiting nutrient in many environments. N is also the most energy expensive for plants to uptake (Galloway et al., 2004; Galloway et al., 2008). Crop production requires large amounts of N fertilizer for maximum yield, especially for cereals, such as maize and rice (Smil, 2001; Godfray et al., 2010; Tilman et al., 2011). However, actual utilization of applied N fertilizer has an efficiency of 50% or less (Raun and Johnson, 1999;

Agtuca MPMI

Edmonds et al., 2013). Thus, improvement in nitrogen use efficiency is needed and essential for sustainable and eco-friendly agriculture.

The overuse of nitrogen fertilizer leads to detrimental soil and environmental consequences. Hence, a major challenge for sustainable agricultural production is how to deliver nitrogen to the plant to maintain high yield, while negating the negative consequences of nitrogen fertilizer addition (Dobermann, 2007; Westhoff, 2009; Sutton et al., 2011). In this context, the use of biological nitrogen fixation (BNF) has often been proposed as one possible solution, at least to reduce, if not to eliminate, the need for heavy N fertilization of non-legume crops (Franche et al., 2009; Lugtenberg and Kamilova, 2009). However, in most situations, the contribution of BNF to growth induced by plant growth promoting bacteria (PGPB) remains unclear or, at least, undefined (Franche et al., 2009; Lugtenberg and Kamilova, 2009).

A variety of BNF bacteria are commonly present in the plant rhizosphere that can establish close associations with roots, colonizing the roots either epiphytically or endophytically. Indeed, PGPB can reach quite high numbers (e.g., 108/g) in roots without inducing a noticeable plant defense response (Reinhold-Hurek and Hurek, 1998, 2011; do Amaral et al., 2017; Faoro et al., 2017). Previous studies showed that PGPB commonly impact root architecture and plant health, attributing these effects to such things as BNF, enhancing stress tolerance, production of phytohormones, enhancing nutrient acquisition, and protection against pathogens and pests (Pérez-Montaño et al., 2014; Pankievicz et al., 2015). Nevertheless, definitive evidence that defines the specific mechanism of PGPB-mediated plant growth promotion remains lacking. In similar plant-microbe interactions (e.g., legume symbiosis), the use of bacterial and/or plant mutants have been

**Agtuca** 

MPMI

particularly useful in defining molecular mechanism. For example, our laboratory recently demonstrated that disruption of the genes for biosynthesis and utilization of poly-3-hydroxybutyrate (PHB), in the endophytic bacterium, *Herbaspirillum seropedicae*, directly affected its ability to promote the growth of *Setaria viridis* (Alves et al., 2019). PHB is a type of polyhdroxyalkanoate (PHA) polymer, produced as a carbon storage compound by a variety of bacterial species. The PHB cycle provides carbon skeletons to synthetic and energetic metabolism, as well as providing reducing power for nitrogen fixation (Lodwig et al., 2005). A few other studies have identified other genes essential for plant growth promotion in other PGPB (Krause et al., 2006; Sessitsch et al., 2012; Shidore et al., 2012; Sarkar and Reinhold-Hurek, 2014). However, while much remains to be done from both the bacterial and plant side, data are particularly missing regarding the molecular

response of the plant host to PGPB association.

In order to define the plant response to PGPB, researchers are applying the full repertoire of modern technologies, including transcriptomics, proteomics, and metabolomics. While the detection of specific transcripts and proteins provides evidence of the potential for a function or pathway to be active, it is only metabolomic analysis that provides definitive evidence that indeed specific metabolism is occurring. There are, for example, specific studies in which metabolomic analysis was nicely integrated into efforts of crop improvement (Zivy et al., 2015; Kumar et al., 2017). Studies in oats, for instance, identified specific metabolic pathways involved with drought tolerance (Sánchez-Martín et al., 2015) and similar efforts identified metabolite-phenotype associations for selecting drought-tolerant ecotypes of *Brachypodium* (Fisher et al., 2016). However, few studies have used metabolomics to investigate PGPB-plant interactions. One example is

Agtuca MPMI

Brusamarello-Santos et al. (2017), who profiled the metabolite distribution of two inbred maize lines upon inoculation with the diazotrophic PGPB, *Azospirillum brasilense* and *Herbaspirillum seropedicae*.

A general limitation with most published metabolomic studies is that they rely on bulk analysis from whole tissues when it is clear, for example, that PGPB colonization of plant roots is highly localized. A diversity of technologies and methodologies are currently available for such a large scale metabolomic analysis, including nuclear magnetic resonance (NMR) spectrometry, gas chromatography-mass spectrometry (GC-MS), liquid chromatography-mass spectrometry (LC-MS), capillary electrophoresis mass spectrometry (CE-MS) and tandem mass spectrometry (Gemperline et al., 2016; Tenenboim and Brotman, 2016; Mhlongo et al., 2018). However, in addition to generally requiring a significant amount of starting plant tissue, these methods are also usually low throughput and do not support *in situ* analysis. Therefore, especially when examining localized areas of PGPB colonization of roots, technologies that allow *in situ* metabolic profiling and imaging of biological tissues via a high throughput approach have clear advantages.

Metabolomic methods that can be performed *in situ* and spatially explicit, commonly suffer from required in-depth and challenging sample preparation procedures. For example, matrix-assisted laser desorption/ionization (MALDI) MS is a method capable of routine, relatively high lateral resolution molecular imaging (10s μm), but requires extensive sample preparation, including the spraying a weak-organic acid onto the sample that assists in facilitating desorption and ionization of molecules (Gemperline et al., 2016; Veličković et al., 2018). In contrast, ambient ionization mass spectrometry-

**Agtuca** 

symbiosis (Agtuca et al., submitted).

MPMI

based approaches, such as laser-ablation electrospray ionization (LAESI), involve minimal sampling methods, while acquiring spatial information of metabolites in biological tissues in their native conditions (Nemes and Vertes, 2007; Nemes et al., 2009; Müller et al., 2011; Stopka et al., 2019). Previously, we demonstrated the utility of using LAESI-MS with ion mobility separation (IMS) to explore the spatial distribution of metabolites in soybean root tissues and nodules infected with BNF rhizobia (Stopka et al., 2017). We also demonstrated that LAESI-MS is useful in identifying the metabolite changes associated with the use of plant and bacterial mutants defective in the soybean-rhizobia

In this study, we demonstrate the utility of LAESI-MS to profile the metabolites associated with localized regions of *Setaria viridis* roots colonized by an endophytic bacterium, *Herbaspirillum seropedicae* SmR1 and, for comparison, a corresponding mutant (SmR54) lacking functional nitrogenase activity (Roncato-Maccari et al., 2003). SmR54 is a *nifA* mutant strain, where NifA functions as a transcriptional activator for *nif* gene expression (Sarkar and Reinhold-Hurek, 2014). This work builds on our previously work, where using nitrogen-13 tracer studies, we showed that *S. viridis*, at least under defined laboratory conditions, obtained a significant amount of its N needs from PGPB-mediated BNF (Pankievicz et al., 2015).

## **RESULTS**

Our past work revealed that co-inoculation of *H. seropedicae* SmR1 and *Azosprillum brasilense* FP2 resulted in significant growth promotion of *S. viridis* with

Agtuca MPMI

measurable incorporation of  $^{13}N_2$  and concomitant shifts in the general abundance of leaf amino acid pools (Pankievicz et al., 2015). A more recent study demonstrated that inoculation of *S. viridis* solely with *H. seropedicae* SmR1 resulted in a significant increase of plant growth within 25 days post-inoculation (Alves et al., 2019). Collectively, these studies demonstrate the ability of *H. seropedicae* to stimulate *S. viridis* growth and the potential for significant effects on plant metabolism. Hence, we focused on this interaction in order to better define the plant metabolomic response, especially at the specific sites of bacterial colonization of the root.

# Bulk metabolomics of S. viridis roots colonized by H. seropedicae.

In order to bolster confidence in our later LAESI-MS analyses, we first used bulk extraction of *S. viridis* plant tissues to sample the metabolome. The experimental samples were derived from two-week-old Setaria plants inoculated with either *H. seropedicae* strain SmR1 (fix<sup>+</sup>) or SmR54 (fix<sup>-</sup>), compared to control uninoculated plants (CTRL). The whole plant roots were ground and extracted in methanol and those samples, with 20 replicates in each sample group, were analyzed by LAESI mass spectrometry (Fig. S1a). Multivariate statistical analysis was performed and showed that all three groups overlapped with no degree of separation according to the Partial Least Squares Discriminant Analysis (PLS-DA) (Fig. S1b). In total, we detected about 130 spectral features with none showing significant differences in abundance based on treatment (Fig. S1c). We interpret these findings to be the result of highly localized zones of bacterial colonization; hence, diluting out any effects that would be infection-site specific.

Agtuca MPMI

# Spatial information in specific root segments colonized by endophytic bacteria.

Instead of bulk analysis, *S. viridis* root segments taken from areas with the highest level of colonization (as shown by GFP) were selected in order to specifically observe the host's response. These samples were then analyzed by LAESI-MS. Again, root segments inoculated with *H. seropedicae* strains SmR1, SmR54, or uninoculated were compared (Fig. S2). Based on GFP expression by the colonizing bacteria, specific root sections were selected, cut, and flash frozen for subsequent LAESI-MS analyses (Fig. 1). As described in Methods, comparable roots were used to quantify the level of bacterial colonization (Fig. S3b), demonstrating that *H. seropedicae* strain SmR1 or SmR54 colonized Setaria roots to equivalent levels. Measurements of root and shoot biomass of inoculated plants, relative to uninoculated plants, showed significant growth promotion regardless of BNF (Fig. S3a), similar to our recently published study (Alves et al., 2019).

Using this approach, six biological replicates in each sample group were examined, where our data showed a clear distinction based on treatment (Fig. 2) in sharp contrast to our bulk analysis (Fig. S1). The heat map (Fig. 2a) showed different metabolic patterns in the CTRL and SmR1 roots. In addition, the CTRL and SmR1 root samples contained the most metabolites that differed in abundance compared to the mutant SmR54 samples (Fig. 2a). Additionally, the PLS-DA scores plot showed a high spectral similarity within sample groups and a high degree of separation among different sample types (Fig. 2b). Component 1 captured the spectral difference between plants that were inoculated (SmR1 and SmR54) and uninoculated. Component 2 reflected spectral differences between plants based on their ability for BNF, i.e., SmR1 relative to CTRL

Agtuca MPMI

and SmR54 root segments (Fig. 2b). A total of 305 spectral features were detected by LAESI-MS between the CTRL and SmR1 roots. Specifically, the CTRL had 12 significantly upregulated metabolites, whereas SmR1 had 15 upregulated metabolites with biological and statistical cutoffs for fold change > 2 and a p-value of < 0.05 (Fig. 2c). When comparing the CTRL and SmR54 roots, 135 spectral features were observed in total. Among these, 27 metabolites were significantly upregulated in the CTRL samples, and 8 were upregulated in the SmR54 roots. Additionally, a total of 281 peaks were detected between roots inoculated with the two bacterial strains, where 59 metabolites were notably abundant in the SmR1 roots and 4 were found upregulated in the SmR54 samples (Fig. 2c). After statistical analyses, there were 36 significantly regulated metabolites with a fold change of at least 2 that were identified (Table 1). Figure 2d shows the box-and-whisker plots for a few of the metabolites that showed significant changes in abundance. For example, glucose phosphate and hydroxyjasmonic acid glucoside were more abundant in the CTRL than in the inoculated roots. Sequovitol was significantly increased in the SmR1 roots relative to the SmR54 and CTRL samples, while norajmaline was more abundant in the SmR54 roots than the other samples (Fig. 2d).

The high abundance of glucose phosphate present in the CTRL roots was expected since it is involved with starch and sucrose metabolism. We assume that carbon metabolism would be affected due to the need for carbon utilization by the colonizing bacteria, especially given the need for energy and reductant to support BNF (Mus et al., 2016). Consistent with our findings, a related study found reduced levels of sugars in PGPB inoculated maize grown hydroponically (da Fonseca Breda et al., 2018). Most of the identified flavonoid metabolites were more abundant in plants inoculated with the

Agtuca MPMI

SmR1 strain, relative to those colonized by the SmR54 mutant (Table 1). This finding is difficult to interpret since flavonoids play a wide variety of roles in plants. For example, these compounds have been shown to serve in signaling and recognition between symbiotic partners (Webster et al., 1998; Balachandar et al., 2006; Shaw et al., 2006; Hardoim et al., 2008). Flavonoids can also modulate internal plant hormone levels, and they may also be signs of plant defense pathway induction (Gough et al., 1997; Subramanian et al., 2007; Tadra-Sfeir et al., 2011; Falcone Ferreyra et al., 2012; Marin et al., 2013; Liu and Murray, 2016). Given the lack of any observable plant defense response and the absence of specific data that flavonoids act as signals to PGPB, we favor the possibility that these flavonoids may be modulating plant metabolism in direct response to colonization. However, at this point, this is merely speculation requiring considerably more work for clarification.

Due to the limitations of our experiments, in some cases we cannot ascertain definitively whether the metabolites detected in the root segments are of plant or bacterial origin. However, we suggest we are primarily analyzing plant metabolites in these samples, given the overall relative mass of the bacterial and plant tissue being analyzed. To further delineate the origin of specific metabolites, it would be necessary to analyze specific plant and/or bacterial mutants blocked in the corresponding pathways. Previously, for example, we used this approach to assign changes in trehalose seen in soybean root hairs to the infecting bacterial symbiont (Brechenmacher et al., 2010).

Allocation of metabolites in the leaves from plants colonized by endophytic PGPB.

Agtuca MPMI

The main focus of our work was to analyze and characterize those metabolites of PGPB colonized roots. However, simultaneously, we took the opportunity to also examine the metabolome of the youngest, newly emerged sink leaf from the same set of plants used for the root analyses (see the PLS-DA scores plot in Fig. 3). We again used six biological replicates for the leaf analyses. Perhaps surprisingly, the comparison of the spectra from the roots and leaves of similarly inoculated and uninoculated plants showed a degree of similarity and separation between plant tissues (Fig. 3). The first component in PLS-DA represented the separation between different types of tissues (root and leaf) from the plants. The second component showed no separation since all of these tissues are from the same plants.

The leaf metabolites significantly more abundant in either the CTRL, SmR1 or SmR54 plant tissues were identified (Table S1). In contrast to roots, there were no detectable differences in the abundance of flavonoid-like compounds in the leaf samples, consistent with the stronger expression of these compounds in roots (Webster et al., 1998). Similarly, consistent with the localization of photosynthesis and starch biosynthesis in leaves, compounds associated with these pathways were more abundant in leaves, irrespective of bacterial strain, with a log<sub>2</sub>(FC) of 1.72, 2.77, and 1.56 for sucrose, ferulyl glucose, and hexose phosphate, respectively (Table S1).

Of note, especially with regard to possible impact on plant growth promotion, we measured high levels of auxin, indole-3-acetic acid (IAA), in the leaves of SmR1 inoculated plants, relative to those from the uninoculated control and SmR54 inoculated plants (Table S1). A number of earlier reports (Lugtenberg and Kamilova, 2009; Spaepen and Vanderleyden, 2011; Monteiro et al., 2012), implicated changes in phytohormone

Agtuca MPMI

levels, especially auxin, as a possible mechanism to explain bacterial plant growth promotion. IAA has a variety of effects in plants, including impacting root branching and vascular development in the shoots (McSteen, 2010). The main auxin biosynthesis pathway is activated when tryptophan converts to IAA in plants, and we found a greater abundance with a log<sub>2</sub>(FC) of 2.08 in the SmR1 than the SmR54 leaves (Table S1). PGPB are capable of synthesizing auxin as well as other plant relevant hormones (Fulchieri et al., 1993; Dobbelaere et al., 2001; Kramer and Bennett, 2006; Baca and Elmerich, 2007; Spaepen and Vanderleyden, 2011). Therefore, our LAESI-MS analysis correlates well with other studies regarding IAA from PGPB in the host. However, note that based on measurements three-weeks after inoculation, strain SmR54, lacking BNF ability, did promote plant growth, similar to strain SmR1 (Fig. S3a). Hence, there is no correlation between the elevated presence of IAA, plant growth promotion and the occurrence of BNF in the roots. It is equally likely that other metabolomic changes, more attributable to BNF, could impact IAA levels in the SmR1-inoculated plants without a measurable impact on plant growth. PGPB can produce auxin but, unlike leaves, significant levels of IAA or tryptophan were not found in the inoculated root segments analyzed, irrespective of BNF (Table S1). Overall, even though the elevation of IAA in the leaves of SmR1-inoculated plants is interesting, we are unable to strongly argue it is playing a key role in bacterial plant growth promotion.

A variety of other metabolites were identified significantly more abundant in either roots or leaves, relative to treatment (Tables S2-S3). These were analyzed by ANOVA with f values ranging from 3 to 130 in SmR1 tissues (Table S2) and 3 to 85 in SmR54 tissues (Table S3).

Metabolic pathways involved in plant growth promotion associated with endophytic bacteria.

After identifying the significant metabolites (Tables 1, S1-S4), their KEGG identification numbers were used for pathway fold enrichment analyses in MetaboAnalyst 4.0 against the rice (*Oryza sativa*) library. Specifically, three-fold enrichment graphs were created: 1) SmR1 versus CTRL tissues (Fig. S4), 2) SmR54 versus CTRL tissues (Fig. S5), and 3) SmR1 versus SmR54 (Fig. 4). Comparing between the SmR1 and CTRL samples, 36 metabolites were used for SmR1 analyses and 20 for the CTRL. Between SmR54 and CTRL samples, there were 28 compounds in the SmR54 and 34 in the CTRL. Additionally, 60 metabolites were used for SmR1 plant tissues and 28 compounds for SmR54. From these analyses, we detected pathways that had a range from 1- to 35-fold enrichment.

There was a total of 15 pathways enriched in the CTRL, 17 in the SmR1, and 8 in the SmR54 roots. Metabolic pathways, including starch and sucrose metabolism, nitrogen metabolism, amino sugar metabolism, and chlorophyll metabolism were highly influenced in the CTRL compared to SmR1 and SmR54 samples as expected (Figs. S4-S5). Even with only 2-weeks of growth, the CTRL and SmR54 plants were slightly N starved since a N source was not provided during growth. However, our previous measurements estimated that only ~7% of the daily nitrogen needs of the plant could be provided by inoculation with wild-type, BNF bacteria (Pankievicz et al., 2015). However, this same study showed that plants grown with bacterial associations under mild nitrogen limiting conditions behaved metabolically and physiologically like normal unstressed plants based

**Agtuca** 

MPMI

on carbon-11 tracer experiments (Pankievicz et al., 2015). Therefore, one must be cautious in attributing specific metabolic differences only to BNF. These comparisons highlight just how difficult it is to have appropriate controls when comparing differing nutrient levels, since nutrient deprivation can have a variety of consequences.

The relative abundance of purine, zeatin, and riboflavin metabolites was significantly higher in the SmR1 and SmR54 inoculated roots, relative to CTRL (Figs. S4-S5). There was ~7- to 11-fold enrichment of purine metabolism in the SmR1 and SmR54 roots, relative to CTRL roots. An explanation for this is not obvious, but may reflect a stimulation of localized plant metabolism, although we also cannot rule out elevation of these compounds due to plant growth. Perhaps more interesting is the elevation of both zeatin and riboflavin in bacterial infected roots, irrespective of BNF (Figs. S4-S5). These data suggest a positive correlation between the elevation of these compounds and measurements of bacterial growth promotion. Zeatin (cytokinin) has a variety of effects on plant growth, including modulating root architecture (Aloni et al., 2006). Cytokinin is a key phytohormone involved in legume nodule formation and elevation in zeatin was detected during soybean root nodulation (Oldroyd and Downie, 2008; Oldroyd et al., 2011; Stopka et al., 2017). There have also been reports in legumes in which rhizobia produced riboflavin was shown to promote plant growth, but riboflavin can also have a variety of other effects (Kanu and Dakora, 2012).

The pathway analyses between SmR1 versus SmR54 were of great interest in order to determine what pathways were affected by BNF (Fig. 4). A total of 11 pathways were detected in the SmR54 roots, and there were 16 in the SmR1 plants. Similar LAESI-MS results using nodulated soybean plants (Agtuca *et al.*, submitted) also found that

Agtuca MPMI

zeatin, purine, and riboflavin metabolism were elevated in plants infected with fix<sup>+</sup> bacteria, relative to those infected with a fix<sup>-</sup> strain. Whereas in plant roots infected with SmR54, pentose and glucuronate, indole alkaloid, pyrimidine, terpenoid biosynthesis, and sugar metabolism were enriched (Fig. 4).

## **DISCUSSION**

The variable and sometimes high cost of N fertilizer (derived from fossil fuels), as well as the detrimental consequences of continued use of high levels of N fertilizer, have led to efforts to enhance the ability to use BNF in non-legume crops. Barriers to the widespread adoption of BNF in such cropping systems are those common to the agricultural use of all biological agents, such as: variability of field-to-field efficacy, competition from endogenous soil organisms, ease of application, etc. An improved understanding of the molecular mechanisms by which PGPB stimulate plant growth, including the potential for BNF to mediate these effects, would contribute to solutions to these practical problems. Efforts to address the questions of molecular mechanism in our lab have included laboratory demonstration that high levels of BNF can be achieved in *S. viridis* when roots were inoculated with an A. brasilense strain specifically engineered to secrete ammonium (Pankievicz et al., 2015). In other work, we also demonstrated the advantages of adopting model grass species for studies of PGPB (Do Amaral et al., 2016), as well as conducted more detailed studies of bacterial genes essential for plant growth promotion (Alves et al., 2019). In the current study, we expanded these investigations by examining metabolic changes that occur at the localized sites of bacterial colonization of S. viridis roots using LAESI-MS analysis.

Agtuca MPMI

Root colonization of *S. viridis* roots by fix<sup>+</sup> and fix<sup>-</sup> endophytic bacteria results in a variety of complex and diverse metabolic changes.

As we demonstrated, bulk analysis of roots colonized by H. seropedicae SmR1 or SmR54, relative to uninoculated plants, failed to detect any significant differences. This is not surprising given that, judging by the distribution of bacterial infection in the root (as visualized by GFP expression), the great majority of the root is not in contact with the bacteria and, hence, may not be responding to any significant level. Dilution of the overall metabolite pool by these non-responding tissues would likely overwhelm any localized responses due to bacterial infection. Thus, the use of an in situ sampling method, such as LAESI-MS, was essential to our ability to detect changes in plant metabolism resulting from PGPB association. Indeed, by this method, there were a number of metabolites whose abundance changed significantly as a result of inoculation with either H. seropedicae SmR1 or SmR54, relative to the uninoculated plants. Collectively, the data clearly show that bacterial inoculation had a dramatic effect on metabolite abundance in general and that BNF also contributed significantly to changes in metabolism. Our findings are consistent with a variety of previous reports that used less localized analyses to conclude that colonization by endophytic bacteria can dramatically affect the plant metabolome and transcriptome, as well as growth (Matilla et al., 2007; Hauberg-Lotte et al., 2012; Shidore et al., 2012; Vacheron et al., 2013; do Amaral et al., 2014; Pankievicz et al., 2015; Aguiar et al., 2016; Pankievicz et al., 2016; Dall'Asta et al., 2017; da Fonseca Breda et al., 2018). Specifically, Brusamarello-Santos et al. (2017) and Sarkar and Reinhold-Hurek (2014) obtained somewhat similar results where there were induced

Agtuca MPMI

changes in abundance and expression between plants that were inoculated with a fix<sup>+</sup> bacterium relative to a fix<sup>-</sup> mutant strain deleted in *nifA*, a transcriptional activator for *nif* genes.

Our previous study used <sup>13</sup>N<sub>2</sub> labeling to show that dual inoculation of *Setaria viridis* plants with wild-type *H. seropedicae* and *A. brasilense* could provide roughly 7% of the N needs of the plant (Pankievicz et al., 2015). However, inoculation with a hyperfixing, ammonium-excreting mutant of *A. brasilense* provided up to 100% of the plant's N needs. This latter result demonstrated the potential for BNF by PGPB to support plant growth. In this same study, changes in general metabolite classes (e.g., amino acids) were determined using carbon-11 radiotracers. The results documented significant shifts in metabolic pools due both to bacterial inoculation and BNF (Pankievicz et al., 2015). An analysis in maize plants inoculated with *H. seropedicae* wild-type SmR1 (fix+) and the BNF defective mutant strain SmR54 (fix-) also documented shifts in both starch and sucrose metabolism in the fix+ plants relative to those not fixing nitrogen (Brusamarello-Santos et al., 2017). Although both of these studies provide results consistent with our findings, the use of LAESI-MS on the specific sites of bacterial colonization provides more specific data and a larger set of differentially affected metabolites.

Although inoculation clearly impacted plant metabolism, a few compounds appeared more abundant in the uninoculated roots. One example is hydroxyjasmonic acid glucoside, which is a component of jasmonic acid biosynthesis (Koch et al., 1997). Jasmonic acid is a well-characterized phytohormone playing key roles in plant development, as well as in the defense response to wounding, abiotic and biotic stress (Liechti and Farmer, 2002; Wasternack, 2007; Wasternack and Hause, 2013; Koo, 2018).

Agtuca MPMI

The elevation of JA-related compounds in the CTRL roots may be due to nitrogen deprivation, but then we would also expect this in the SmR54 infected roots, which was not seen in our analysis. Hydroxyjasmonic acid glucoside is a glycosidic conjugate formed during jasmonic acid biosynthesis (Widemann et al., 2013) and its formation switches off jasmonic acid signaling (Miersch et al., 2008). However, we cannot rule out other functions for this compound in plant metabolism. It is interesting to speculate that the higher abundance of hydroxyjasmonic acid glucoside in CTRL roots is a reflection of the lack of infection, with hydrolysis of this compound occurring in roots upon PGPB infection. The interplay of specific phytohormones, plant defense pathways, and plant growth is complex but could be a significant contributor to PGPB-induced plant growth.

Sequoyitol was detected and more abundant in the SmR1 roots with a log2(FC) of 2.15 and 1.43, relative to the SmR54 and CTRL root samples (Table 1). However, there is little data on the function of this metabolite in plants. Sequoyitol is a cyclitol, which may function as an osmolyte or osmoprotectant (Ford, 1984), as well as a carbon storage compound in plants (Richter and Popp, 1992). It was shown that cyclitols increase in abundance in both legumes and non-legumes in response to drought and other abiotic stresses (Ford, 1984; Keller and Ludlow, 1993; Guo and Oosterhuis, 1995, 1997; Wanek and Richter, 1997; Streeter et al., 2001). Regarding nitrogen-fixing, symbiotic associations, cyclitols, including sequoyitol, are abundant in the infected cells within the central region of soybean root nodules (Streeter and Bosler, 1976; Streeter, 1980; Phillips et al., 1982). However, their specific role in nodule metabolism remains undefined.

Agtuca MPMI

Intersections between the metabolome of PGPB-infected roots and plant innate immunity.

Roots colonized by the SmR1 strain had an abundance of ajmaline and norajmaline, relative to roots infected by the wild-type SmR54 or CTRL samples. Aimaline, noraimaline, and related compounds (vinblastine, vincristine, vindoline) are involved in terpenoid indole alkaloid (TIA) biosynthesis that occurs in a jasmonateresponsive manner and has been studied in a variety of plant systems, including Rauvolfia serpentine and Catharanthus roseus (St-Pierre et al., 1999; Facchini and St-Pierre, 2005; Facchini and De Luca, 2008; Guirimand et al., 2011). These alkaloid metabolites are low-molecular-weight, heterocyclic compounds and have been studied in large part due to their pharmacological activities (Jacobs et al., 2004; Verma et al., 2012). However, these compounds are present in plants in low amount making them expensive to purify from plant tissues. Studies have focused on finding ways to increase the accumulation of these metabolites for therapeutic and pharmaceutical uses (Jacobs et al., 2004). However, they appear to be absent in most plants, including the well-studied model system, Arabidopsis (Van Moerkercke et al., 2013). There are examples. nonetheless, where infection by fungal endophytes, such as those infecting *C. roseus*. significantly enhances terpenoid biosynthesis (Kumar et al., 2013; Tiwari et al., 2013; Pandey et al., 2016). In these specific situations, the presence of the fungal endophyte also significantly affects plant growth, as well as stress tolerance. Hence, it is intriguing that higher levels of such terpenoid compounds were found in Setaria roots after PGPB inoculation, although clearly the data do not establish cause and effect between these compounds and growth promotion. However, here again, a perfect correlation is not found

**Agtuca** 

MPMI

since it was the roots infected by the SmR54 strain that showed the highest elevation of TIA abundance (i.e., 7-10 fold), while both the SmR1 and SmR54 inoculated plants showed measurable effects on plant growth.

If one reads reviews on the legume-rhizobial symbiosis, as well as articles describing associative (PGPB) associations, one might get the impression that the former is quite complex, while the latter can be explained by relatively simple changes (e.g., in auxin or cytokinin levels) (Oldroyd and Downie, 2008; Lugtenberg and Kamilova, 2009; Oldroyd et al., 2011; Chagas et al., 2018). However, a major conclusion from our study is that colonization of Setaria roots by *H. seropedicae* elicits a large variety of complex metabolic changes suggesting the bacteria may have the ability to exploit the plant in specific ways to support its growth and stability. In this way, the interaction of PGPB with plants would not be that different, in a general sense, from other plant-microbe interactions, many of which have been studied in far greater detail than PGPB-plant associations. With regard to plant symbionts, PGPB are also similar to rhizobia in that they can colonize the root to guite high, numerical levels without the induction of a visible plant defense response. Our metabolomics data confirms the absence of many metabolites one would associate with plant defense, although it is not clear that PGPB are totally benign to the plant. Since our laboratory has also conducted metabolite profiling of soybean root nodules, we compared and contrasted the results of these studies (Agtuca et al., submitted). There are clear similarities. For example, both systems show a significant impact on auxin, purine, zeatin, riboflavin, and starch and sucrose metabolism, as well as induction of flavonoid accumulation. We are still in the very early stages of understanding the complexity of PGPB infection, establishment, and function in

Agtuca MPMI

plants, especially in comparison to the wealth of knowledge available on the legume symbiosis.

## **MATERIALS AND METHODS**

## Bacterial culture conditions.

*H. seropedicae* SmR1 (fix<sup>+</sup>) and SmR54 (fix<sup>-</sup>) strains were grown in NFbHP-malate liquid medium that contained 20 mL L<sup>-1</sup> of NH<sub>4</sub>Cl as the nitrogen source (Klassen et al., 1997) at 30 °C and 130 RPM overnight. Streptomycin at a final concentration of 80 μg ml<sup>-1</sup> and Kanamycin at a final concentration of 200 μg ml<sup>-1</sup> were added to the medium. Once the cultures reached an OD<sub>600</sub> of 1.0 (10<sup>8</sup> cells ml<sup>-1</sup>), the bacteria were pelleted and washed 3 times with 0.9% of NaCl solution. The bacterial suspension was diluted to 10<sup>7</sup> cells ml<sup>-1</sup> and 1 ml per seedling was used for inoculation.

# Plant growth and inoculation.

Setaria viridis A10.1 seeds were pre-treated with sulfuric acid for 15 min. Seeds were then rinsed with water and sterilized with 1% (v/v) bleach plus 0.1% (v/v) Tween 20 for 3 min and washed 3× with sterile deionized water. The seeds were transferred and germinated on Hoagland's solution on 1% (w/v) phytagel agar (Hoagland and Arnon, 1950). Seeds were incubated at 30 °C for 1 day in the dark, followed by 2 days in the light. At three days post germination, seedlings were soaked in either SmR1 or SmR54 bacterial suspensions for 30 min. The control seedlings were soaked in sterile Hoagland's

**Agtuca** 

MPMI

solution with no inoculum. Upon inoculation, all seedlings from different sample groups (CTRL, SmR1, SmR54) were planted in soil comprised of a 3:1 Turface:Vermiculite mixture, respectively. The Setaria plants grew for 2 weeks post-inoculation after which they were either observed by microscopy or rapidly frozen in liquid nitrogen for subsequent extraction for bulk or LAESI-MS metabolomic analyses. A subset of the roots was also used to measure the level of bacterial colonization. Some plants from the same batch were grown for an additional week in order to quantify plant growth promotion.

# Confocal and fluorescence imaging of root colonization.

H. seropedicae SmR1 (fix\*) and SmR54 (fix\*), both constitutively expressing GFP, were used to identify areas of bacterial colonization in the roots of *S. viridis* A10.1. The control and inoculated roots were placed on a slide separately with a drop of water, which was covered with a glass coverslip to view either using a laser scanning confocal microscope or fluorescence microscope (Zeiss Axiovert 200M) with Leica DFC290 color camera. The roots were closely examined in order to define a segment with the highest level of endophytic bacterial colonization (as judged by GFP). Bright and fluorescence images were obtained and overlaid in the Metamorph v.7.8.12 software program. After imaging, 20 root segments of ~1 cm in length were harvested from 10 different roots, frozen in liquid nitrogen, and stored at -80 °C until LAESI analysis. Each segment represents a biological replicate. A similar number of root segments from roughly the same regions of the root were harvested from uninoculated plants to serve as the control. Shoots from 10 different plants, but from the same set of plants used to harvest the root

Agtuca MPMI

tissue, were also harvested, frozen in liquid nitrogen, and stored at -80 °C until LAESI analysis.

## **LAESI-MS** instrumentation.

The instrumentation was similar as for our previous paper (Stopka et al., 2017). A mid-IR laser (IR OpoletteHE 2731, Opotek, Carlsbad, CA, USA) operating at 2.94 µm wavelength and 20 Hz repetition rate was used for direct ablation of the root segments. The laser beam was steered using gold-coated mirrors through a 50-mm focal length plano-convex CaF<sub>2</sub> focusing lens. The frozen root segments were placed onto a microscope slide on an automated XY stage (MLS203-1, Thorlabs, Newton, NJ, USA) in direct line with the focused laser beam. An ablation plume of neutrals was produced as the root segment was targeted, which was then ionized by an electrospray and the ions where sampled by the mass spectrometer that was operating in negative ion mode (see Fig. 1). The electrospray solvent composition was 2:1 (v/v) MeOH:CHCl<sub>3</sub> and was dispensed at a flow rate of 500 nL/min through a stainless steel emitter held at 2.7 kV spray voltage. For targeted ablation a side microscope (AM4815ZTL, Dino-lite, Torrance, CA, USA) was used to ensure the whole root segment was ablated and the sample was correctly positioned using the automated stage.

## Setaria viridis bulk analyses.

Approximately 10 mg of frozen root tissue from the control and inoculated plants were homogenized for LAESI-MS bulk analyses. The tissues were placed into 2 mL

**Agtuca** 

MPMI

Eppendorf tubes and suspended with 40 μL of DI water. The samples were probe

sonicated (QSonica Q125, Newton, CT, USA), for 30 sec with 1 sec pulse durations, at an amplitude of 30% while on ice. Approximately 10 µL of the sonicated material was placed on a glass microscope slide for LAESI-MS analysis.

## Metabolic profiling of plant tissues and bacterial pellets.

After fluorescence imaging, the harvested, root segments with the highest endophytic colonization (SmR1 and SmR54) and uninoculated segments (n = 6) were analyzed by LAESI-MS. For the leaf analyses from the inoculated and uninoculated plants, the frozen leaves (same set of plants as analyzed from the root segments by fluorescence imaging) were observed and out of the 3 developed leaves on each plant, the youngest, newly emerged sink leaf was selected, cut to ~1 cm in length, and used for *in situ* metabolic profiling. The frozen selected tissues, including the sink leaf and root segments, were placed on a microscope slide and 2 sec later 2  $\mu$ L of sterile water was added on top of the root segments in order to have higher water content for LAESI-MS ablation. After 10-20 sec from when the samples were placed on the microscope slide, the leaves and the hydrated root segments were then analyzed by LAESI-MS. A laser energy of ~1.5 mJ per pulse with a 20 Hz repetition rate was used to ablate the plant tissues in a raster formation.

Free-living cultures of *H. seropedicae* SmR1 (fix<sup>+</sup>) wildtype and SmR54 fix<sup>-</sup> mutant strains were grown in the appropriate medium as stated in the bacterial culture conditions section. These bacteria were then sub-cultured and grown overnight in NFbHP-malate

MPMI

medium that had 20 ml L<sup>-1</sup> of NH<sub>4</sub>Cl as a nitrogen source without antibiotics until reaching an  $OD_{600}$  = 1.0 (10<sup>8</sup> cells mL<sup>-1</sup>). The bacterial cultures were centrifuged at 5,000 rpm for 2 min and washed with sterile water. This was repeated a total of 3-times. After washing, the bacterial pellets were resuspended in 20 µL of deionized water. The suspended pellet (10 µL) was placed onto a microscope glass slide. Six biological replicates of the suspended pellets were analyzed by LAESI-MS.

**Agtuca** 

# Biomass measurements and bacterial colonization assay.

Plant roots at 2 weeks after inoculation were used to measure the level of bacterial colonization. Fresh roots were macerated in 1 mL of 0.9% (w/v) NaCl solution. The homogenized roots were then serially diluted and 10 µL of the final dilution were plated on solid NFbHP-malate medium with addition of the respective antibiotics. Plates were incubated for 3 days at 30 °C and colony-forming units (CFU) were counted and converted into CFU g<sup>-1</sup> of fresh tissue.

The remaining plants grown for 3 weeks after inoculation were dried completely in a 45 °C incubator for biomass measurements. Roots and shoots were weighed separately. Total biomass was calculated by summing the two dry weight measurements.

## Metabolite identification.

In order to obtain a library of *S. viridis* root and leaf metabolites, 10 plants were grown as described above and their leaves and whole roots harvested, flash frozen in

Agtuca MPMI

liquid nitrogen and stored at -80 °C until use. Approximately 1 g of the frozen root and leaf tissues were ground separately by mortar and pestle in liquid nitrogen until a fine powder was obtained. The ground samples were transferred to 1.5 mL Eppendorf tubes and resuspended in 2:1 (v/v) chloroform:methanol solution. The samples were vortexed and centrifuged at 5000×g for 5 min at room temperature. Then, the supernatant was transferred to a new 1.5 mL Eppendorf tube. The samples were centrifuged two more times in order to have a clear supernatant extract. These extracts were then transferred to a 500 µL Hamilton syringe for electrospray ionization tandem mass spectrometry (ESI-MS/MS) analyses. A syringe pump was used to drive the syringe that included the prepared lysates. In addition, the syringe was connected to a stainless-steel emitter (MT320-50-5-5, New Objective, Woburn, MA) through a fused silica tube. The flow rate of the syringe pump was at 500 nL/min and the prepared solution was sprayed by employing a spraying voltage of -2200 V to the emitter. A Q-TOF mass spectrometer (Synapt G2S, Waters, Milford, MA) was used to analyze the generated ions. Significant metabolites previously detected by LAESI-MS were chosen for tandem MS by collision induced dissociation (CID) with collision energies from 10 to 50 eV. The Metabolite Standard Initiative (MSI) levels for metabolite identification were implemented for peak assignments. All steps for metabolite identification were adapted from our previous study (Stopka et al., 2017).

# Data and statistical analyses.

After LAESI-MS analyses, the raw mass spectra from plant samples and bacterial pellets with six biological replicates were processed by averaging ten MS scans and

Agtuca MPMI

subtracting the background from equal numbers of ESI only scans. The processed data were analyzed by MetaboAnalyst 4.0, a web-based metabolomic processing software, using univariate, multivariate, and hierarchical clustering statistical approaches. The data were normalized as described in the supporting methods from Stopka et al. (2017). Heat maps, PLS-DA scores and loading plots, and box-and-whisker plots were constructed by MetaboAnalyst 4.0. Volcano plots were also generated for all detected ions and the significant ions with a p < 0.05 and a fold change of > 2 were highlighted based on Student's t-test. The pathway analyses were conducted by MetaboAnalyst 4.0. The rice (*Oryza sativa*) pathways were downloaded from KEGG (https://www.genome.jp/kegg/) and were used in the pathway enrichment analysis as the reference set.

# **ACKNOWLEDGMENTS**

The material is based work supported by the U.S. Department of Energy (DOE), Office of Biological and Environmental Research (OBER) under award number DE-SC0013978 and National Science Foundation (NSF) Plant Genome Program under award number IOS-1734145. We thank Frank Baker and Alexander Jurkevich from the Molecular Cytology Core at the C. S. Bond Life Sciences Center, the University of Missouri and Will Chrisler from EMSL for their help on the microscope images. We acknowledge Marina Cotta and Tomas Pellizzaro Pereira for help with growing Setaria plants. We thank J. Robil for the graphic design of Fig. 1. B.J.A. would like to thank the U.S. DOE Mickey Leland Energy Fellowship and the University of Missouri's College of Agriculture, Food and Natural Resources (CAFNR) and Office of Graduate Studies for the George Washington Carver Fellowship and Gus T. Ridgel Fellowship. S.E. was

MPMI

supported by the University of Missouri's Freshman Research in Plant Sciences (FRIPS)

632 program.

**Agtuca** 

## **AUTHOR CONTRIBUTIONS**

- B.J.A., S.A.S, A.V., and G.S. designed the experiments. B.J.A., S.A.S., T.R.T. and S.E.,
- performed the research. B.J.A., S.A.S., S.E., Y.L., and D.X. analyzed the data. B.J.A.
- wrote the article with input from F.P.A., S.A.S., S.E., D.X., R.A.M., D.W.K., L.P., C.R.A.,
- 638 A.V., and G.S.

## LITERATURE CITED

- Aguiar, N., Medici, L., Olivares, F., Dobbss, L., Torres-Netto, A., Silva, S., Novotny, E., and Canellas, L. 2016. Metabolic profile and antioxidant responses during drought stress recovery in sugarcane treated with humic acids and endophytic diazotrophic bacteria. Annals of applied biology 168:203-213.
- Aloni, R., Aloni, E., Langhans, M., and Ullrich, C. 2006. Role of cytokinin and auxin in shaping root architecture: regulating vascular differentiation, lateral root initiation, root apical dominance and root gravitropism. Annals of botany 97:883-893.
- Alves, L.P.S., do Amaral, F.P., Kim, D., Bom, M.T., Gavídia, M.P., Teixeira, C.S., Holthman, F., de Oliveira Pedrosa, F., de Souza, E.M., and Chubatsu, L.S. 2019. Importance of poly-3-hydroxybutyrate (PHB) metabolism to the ability of Herbaspirillum seropedicae to promote plant growth. Appl. Environ. Microbiol.:AEM. 02586-02518.
- Baca, B., and Elmerich, C. 2007. Microbial production of plant hormones. Pages 113-143 in: Associative and endophytic nitrogen-fixing bacteria and cyanobacterial associations. Springer.
- Balachandar, D., Sandhiya, G., Sugitha, T., and Kumar, K. 2006. Flavonoids and growth hormones influence endophytic colonization and in planta nitrogen fixation by a diazotrophic Serratia sp. in rice. World Journal of Microbiology and Biotechnology 22:707-712.
- Brechenmacher, L., Lei, Z., Libault, M., Findley, S., Sugawara, M., Sadowsky, M.J., Sumner, L.W., and Stacey, G. 2010. Soybean metabolites regulated in root hairs in response to the symbiotic bacterium Bradyrhizobium japonicum. Plant Physiology 153:1808-1822.
- Brusamarello-Santos, L.C., Gilard, F., Brulé, L., Quilleré, I., Gourion, B., Ratet, P., De Souza, E.M., Lea, P.J., and Hirel, B. 2017. Metabolic profiling of two maize (Zea

Agtuca MPMI

mays L.) inbred lines inoculated with the nitrogen fixing plant-interacting bacteria Herbaspirillum seropedicae and Azospirillum brasilense. PloS one 12:e0174576.

- Chagas, F.O., de Cassia Pessotti, R., Caraballo-Rodríguez, A.M., and Pupo, M.T. 2018. Chemical signaling involved in plant–microbe interactions. Chemical Society Reviews 47:1652-1704.
- da Fonseca Breda, F.A., da Silva, T.F.R., dos Santos, S.G., Alves, G.C., and Reis, V.M. 2018. Modulation of nitrogen metabolism of maize plants inoculated with Azospirillum brasilense and Herbaspirillum seropedicae. Archives of Microbiology:1-12.
- Dall'Asta, P., Pereira, T.P., Do Amaral, F.P., and Arisi, A.C.M. 2017. Tools to evaluate Herbaspirillum seropedicae abundance and nifH and rpoC expression in inoculated maize seedlings grown in vitro and in soil. Plant growth regulation 83:397-408.
- do Amaral, F.P., Agtuca, B.J., and Stacey, G. 2017. Setaria Root–Microbe Interactions. Pages 239-250 in: Genetics and Genomics of Setaria, Springer.
- do Amaral, F.P., Bueno, J.C.F., Hermes, V.S., and Arisi, A.C.M. 2014. Gene expression analysis of maize seedlings (DKB240 variety) inoculated with plant growth promoting bacterium Herbaspirillum seropedicae. Symbiosis 62:41-50.
- do Amaral, F.P., Pankievicz, V.C., Arisi, A.C.M., de Souza, E.M., Pedrosa, F., and Stacey, G. 2016. Differential growth responses of Brachypodium distachyon genotypes to inoculation with plant growth promoting rhizobacteria. Plant molecular biology 90:689-697.
- Dobbelaere, S., Croonenborghs, A., Thys, A., Ptacek, D., Vanderleyden, J., Dutto, P., Labandera-Gonzalez, C., Caballero-Mellado, J., Aguirre, J.F., and Kapulnik, Y. 2001. Responses of agronomically important crops to inoculation with Azospirillum. Functional Plant Biology 28:871-879.
- Dobermann, A. 2007. Nutrient use efficiency—measurement and management. Fertilizer best management practices 1.
- Edmonds, D.E., Tubaña, B.S., Kelly, J.P., Crain, J.L., Edmonds, M.D., Solie, J.B., Taylor, R.K., and Raun, W.R. 2013. Maize grain yield response to variable row nitrogen fertilization. Journal of plant nutrition 36:1013-1024.
- Facchini, P.J., and St-Pierre, B. 2005. Synthesis and trafficking of alkaloid biosynthetic enzymes. Current opinion in plant biology 8:657-666.
- Facchini, P.J., and De Luca, V. 2008. Opium poppy and Madagascar periwinkle: model non-model systems to investigate alkaloid biosynthesis in plants. The Plant Journal 54:763-784.
- Falcone Ferreyra, M.L., Rius, S., and Casati, P. 2012. Flavonoids: biosynthesis, biological functions, and biotechnological applications. Frontiers in plant science 3:222.
- Faoro, H., Rene Menegazzo, R., Battistoni, F., Gyaneshwar, P., do Amaral, F.P., Taulé, C., Rausch, S., Gonçalves Galvão, P., de los Santos, C., and Mitra, S. 2017. The oil-contaminated soil diazotroph Azoarcus olearius DQS-4T is genetically and phenotypically similar to the model grass endophyte A zoarcus sp. BH 72. Environmental microbiology reports 9:223-238.
- Fisher, L.H., Han, J., Corke, F.M., Akinyemi, A., Didion, T., Nielsen, K.K., Doonan, J.H., Mur, L.A., and Bosch, M. 2016. Linking dynamic phenotyping with metabolite

**Agtuca** 

**MPMI** 

- analysis to study natural variation in drought responses of Brachypodium distachyon. Frontiers in plant science 7:1751.
- Ford, C.W. 1984. Accumulation of low molecular weight solutes in water-stressed tropical legumes. Phytochemistry 23:1007-1015.
- Franche, C., Lindström, K., and Elmerich, C. 2009. Nitrogen-fixing bacteria associated with leguminous and non-leguminous plants. Plant and soil 321:35-59.
- Fulchieri, M., Lucangeli, C., and Bottini, R. 1993. Inoculation with Azospirillum lipoferum affects growth and gibberellin status of corn seedling roots. Plant and Cell physiology 34:1305-1309.
- Galloway, J.N., Townsend, A.R., Erisman, J.W., Bekunda, M., Cai, Z., Freney, J.R., Martinelli, L.A., Seitzinger, S.P., and Sutton, M.A. 2008. Transformation of the nitrogen cycle: recent trends, questions, and potential solutions. Science 320:889-892.
- Galloway, J.N., Dentener, F.J., Capone, D.G., Boyer, E.W., Howarth, R.W., Seitzinger, S.P., Asner, G.P., Cleveland, C.C., Green, P., and Holland, E.A. 2004. Nitrogen cycles: past, present, and future. Biogeochemistry 70:153-226.
- Gemperline, E., Keller, C., and Li, L. (2016). Mass spectrometry in plant-omics (ACS Publications).
- Godfray, H.C.J., Beddington, J.R., Crute, I.R., Haddad, L., Lawrence, D., Muir, J.F., Pretty, J., Robinson, S., Thomas, S.M., and Toulmin, C. 2010. Food security: the challenge of feeding 9 billion people. science 327:812-818.
- Gough, C., Galera, C., Vasse, J., Webster, G., Cocking, E.C., and Dénarié, J. 1997. Specific flavonoids promote intercellular root colonization of Arabidopsis thaliana by Azorhizobium caulinodans ORS571. Molecular plant-microbe interactions 10:560-570.
- Guirimand, G., Guihur, A., Poutrain, P., Héricourt, F., Mahroug, S., St-Pierre, B., Burlat, V., and Courdavault, V. 2011. Spatial organization of the vindoline biosynthetic pathway in Catharanthus roseus. Journal of plant physiology 168:549-557.
- Guo, C., and Oosterhuis, D.M. 1995. Pinitol occurrence in soybean plants as affected by temperature and plant growth regulators. Journal of Experimental Botany 46:249-253.
- Guo, C., and Oosterhuis, D.M. 1997. Effect of water-deficit stress and genotypes on pinitol occurrence in soybean plants. Environmental and experimental botany 37:147-152.
- Hardoim, P.R., van Overbeek, L.S., and van Elsas, J.D. 2008. Properties of bacterial endophytes and their proposed role in plant growth. Trends in microbiology 16:463-471.
- Hauberg-Lotte, L., Klingenberg, H., Scharf, C., Böhm, M., Plessl, J., Friedrich, F., Völker, U., Becker, A., and Reinhold-Hurek, B. 2012. Environmental factors affecting the expression of pilAB as well as the proteome and transcriptome of the grass endophyte Azoarcus sp. strain BH72. PLoS One 7:e30421.
- Hoagland, D.R., and Arnon, D.I. 1950. The water-culture method for growing plants without soil. Circular. California agricultural experiment station 347.
- Jacobs, D.I., Snoeijer, W., Hallard, D., and Verpoorte, R. 2004. The Catharanthus alkaloids: pharmacognosy and biotechnology. Current medicinal chemistry 11:607-628.

Agtuca MPMI

Kanu, S.A., and Dakora, F.D. 2012. Effect of N and P nutrition on extracellular secretion of lumichrome, riboflavin and indole acetic acid by N 2-fixing bacteria and endophytes isolated from Psoralea nodules. Symbiosis 57:15-22.

- Keller, F., and Ludlow, M. 1993. Carbohydrate metabolism in drought-stressed leaves of pigeonpea (Cajanus cajan). Journal of Experimental Botany 44:1351-1359.
- Klassen, G., Pedrosa, F., Souza, E., Funayama, S., and Rigo, L. 1997. Effect of nitrogen compounds on nitrogenase activity in Herbaspirillum seropedicae SMR1. Canadian journal of microbiology 43:887-891.
- Koch, T., Bandemer, K., and Boland, W. 1997. Biosynthesis of cis-jasmone: a pathway for the inactivation and the disposal of the plant stress hormone jasmonic acid to the gas phase? Helvetica Chimica Acta 80:838-850.
- Koo, A.J. 2018. Metabolism of the plant hormone jasmonate: a sentinel for tissue damage and master regulator of stress response. Phytochem. Rev. 17:51-80.
- Kramer, E.M., and Bennett, M.J. 2006. Auxin transport: a field in flux. Trends in plant science 11:382-386.
- Krause, A., Ramakumar, A., Bartels, D., Battistoni, F., Bekel, T., Boch, J., Böhm, M., Friedrich, F., Hurek, T., and Krause, L. 2006. Complete genome of the mutualistic, N 2-fixing grass endophyte Azoarcus sp. strain BH72. Nature biotechnology 24:1384.
- Kumar, A., Patil, D., Rajamohanan, P.R., and Ahmad, A. 2013. Isolation, purification and characterization of vinblastine and vincristine from endophytic fungus Fusarium oxysporum isolated from Catharanthus roseus. PloS one 8:e71805.
- Kumar, R., Bohra, A., Pandey, A.K., Pandey, M.K., and Kumar, A. 2017. Metabolomics for Plant Improvement: Status and Prospects. Frontiers in Plant Science 8.
- Liechti, R., and Farmer, E.E. 2002. The jasmonate pathway. Science 296:1649-1650.
- Liu, C.-W., and Murray, J. 2016. The role of flavonoids in nodulation host-range specificity: an update. Plants 5:33.
- Lodwig, E., Leonard, M., Marroqui, S., Wheeler, T., Findlay, K., Downie, J., and Poole, P. 2005. Role of polyhydroxybutyrate and glycogen as carbon storage compounds in pea and bean bacteroids. Molecular plant-microbe interactions 18:67-74.
- Lugtenberg, B., and Kamilova, F. 2009. Plant-growth-promoting rhizobacteria. Annual review of microbiology 63:541-556.
- Marin, A., Souza, E., Pedrosa, F., Souza, L., Sassaki, G., Baura, V., Yates, M., Wassem, R., and Monteiro, R. 2013. Naringenin degradation by the endophytic diazotroph Herbaspirillum seropedicae SmR1. Microbiology 159:167-175.
- Matilla, M.A., Espinosa-Urgel, M., Rodríguez-Herva, J.J., Ramos, J.L., and Ramos-González, M.I. 2007. Genomic analysis reveals the major driving forces of bacterial life in the rhizosphere. Genome biology 8:R179.
- McSteen, P. 2010. Auxin and monocot development. Cold Spring Harbor perspectives in biology 2:a001479.
- Mhlongo, M.I., Piater, L.A., Madala, N.E., Labuschagne, N., and Dubery, I.A. 2018. The chemistry of plant—microbe interactions in the rhizosphere and the potential for metabolomics to reveal signaling related to defense priming and induced systemic resistance. Frontiers in plant science 9:112.
- Miersch, O., Neumerkel, J., Dippe, M., Stenzel, I., and Wasternack, C. 2008. Hydroxylated jasmonates are commonly occurring metabolites of jasmonic acid

 **Agtuca** 

and contribute to a partial switch-off in jasmonate signaling. New Phytologist

and contribute to a partial switch-off in jasmonate signaling. New Phytologist 177:114-127.

MPMI

- Monteiro, R.A., Balsanelli, E., Wassem, R., Marin, A.M., Brusamarello-Santos, L.C., Schmidt, M.A., Tadra-Sfeir, M.Z., Pankievicz, V.C., Cruz, L.M., and Chubatsu, L.S. 2012. Herbaspirillum-plant interactions: microscopical, histological and molecular aspects. Plant and Soil 356:175-196.
- Müller, T., Oradu, S., Ifa, D.R., Cooks, R.G., and Kräutler, B. 2011. Direct plant tissue analysis and imprint imaging by desorption electrospray ionization mass spectrometry. Analytical chemistry 83:5754-5761.
- Mus, F., Crook, M.B., Garcia, K., Costas, A.G., Geddes, B.A., Kouri, E.D., Paramasivan, P., Ryu, M.-H., Oldroyd, G.E., and Poole, P.S. 2016. Symbiotic nitrogen fixation and the challenges to its extension to nonlegumes. Appl. Environ. Microbiol. 82:3698-3710.
- Nemes, P., and Vertes, A. 2007. Laser ablation electrospray ionization for atmospheric pressure, in vivo, and imaging mass spectrometry. Analytical chemistry 79:8098-8106.
- Nemes, P., Barton, A.A., and Vertes, A. 2009. Three-dimensional imaging of metabolites in tissues under ambient conditions by laser ablation electrospray ionization mass spectrometry. Analytical Chemistry 81:6668-6675.
- Oldroyd, G.E., and Downie, J.A. 2008. Coordinating nodule morphogenesis with rhizobial infection in legumes. Annu. Rev. Plant Biol. 59:519-546.
- Oldroyd, G.E., Murray, J.D., Poole, P.S., and Downie, J.A. 2011. The rules of engagement in the legume-rhizobial symbiosis. Annual review of genetics 45:119-144.
- Pandey, S.S., Singh, S., Babu, C.V., Shanker, K., Srivastava, N., Shukla, A.K., and Kalra, A. 2016. Fungal endophytes of Catharanthus roseus enhance vindoline content by modulating structural and regulatory genes related to terpenoid indole alkaloid biosynthesis. Scientific reports 6:26583.
- Pankievicz, V., Camilios-Neto, D., Bonato, P., Balsanelli, E., Tadra-Sfeir, M., Faoro, H., Chubatsu, L., Donatti, L., Wajnberg, G., and Passetti, F. 2016. RNA-seq transcriptional profiling of Herbaspirillum seropedicae colonizing wheat (Triticum aestivum) roots. Plant molecular biology 90:589-603.
- Pankievicz, V.C., do Amaral, F.P., Santos, K.F., Agtuca, B., Xu, Y., Schueller, M.J., Arisi, A.C.M., Steffens, M.B., de Souza, E.M., and Pedrosa, F.O. 2015. Robust biological nitrogen fixation in a model grass—bacterial association. The Plant Journal 81:907-919.
- Pérez-Montaño, F., Alías-Villegas, C., Bellogín, R., Del Cerro, P., Espuny, M., Jiménez-Guerrero, I., López-Baena, F.J., Ollero, F., and Cubo, T. 2014. Plant growth promotion in cereal and leguminous agricultural important plants: from microorganism capacities to crop production. Microbiological research 169:325-336.
- Phillips, D.V., Dougherty, D.E., and Smith, A.E. 1982. Cyclitols in soybean. Journal of agricultural and food chemistry 30:456-458.
- Raun, W.R., and Johnson, G.V. 1999. Improving nitrogen use efficiency for cereal production. Agronomy journal 91:357-363.

Agtuca MPMI

Reinhold-Hurek, B., and Hurek, T. 1998. Life in grasses: diazotrophic endophytes. Trends in microbiology 6:139-144.

- Reinhold-Hurek, B., and Hurek, T. 2011. Living inside plants: bacterial endophytes. Current opinion in plant biology 14:435-443.
- Richter, A., and Popp, M. 1992. The physiological importance of accumulation of cyclitols in Viscum album L. New Phytologist 121:431-438.
- Roncato-Maccari, L.D.B., Ramos, H.J.O., Pedrosa, F.O., Alquini, Y., Chubatsu, L.S., Yates, M.G., Rigo, L.U., Steffens, M.B.R., and Souza, E.M. 2003. Endophytic Herbaspirillum seropedicae expresses nif genes in gramineous plants. Fems Microbiology Ecology 45:39-47.
- Sánchez-Martín, J., Heald, J., Kingston-Smith, A., Winters, A., Rubiales, D., Sanz, M., Mur, L.A., and Prats, E. 2015. A metabolomic study in oats (A vena sativa) highlights a drought tolerance mechanism based upon salicylate signalling pathways and the modulation of carbon, antioxidant and photo-oxidative metabolism. Plant, Cell & Environment 38:1434-1452.
- Sarkar, A., and Reinhold-Hurek, B. 2014. Transcriptional profiling of nitrogen fixation and the role of NifA in the diazotrophic endophyte Azoarcus sp. strain BH72. PLoS One 9:e86527.
- Sessitsch, A., Hardoim, P., Döring, J., Weilharter, A., Krause, A., Woyke, T., Mitter, B., Hauberg-Lotte, L., Friedrich, F., and Rahalkar, M. 2012. Functional characteristics of an endophyte community colonizing rice roots as revealed by metagenomic analysis. Molecular Plant-Microbe Interactions 25:28-36.
- Shaw, L.J., Morris, P., and Hooker, J.E. 2006. Perception and modification of plant flavonoid signals by rhizosphere microorganisms. Environmental Microbiology 8:1867-1880.
- Shidore, T., Dinse, T., Öhrlein, J., Becker, A., and Reinhold-Hurek, B. 2012. Transcriptomic analysis of responses to exudates reveal genes required for rhizosphere competence of the endophyte Azoarcus sp. strain BH72. Environmental Microbiology 14:2775-2787.
- Smil, V. 2001. Fritz Haber, Carl Bosch and the transformation of world food production. Enriching the Earth:128-131.
- Spaepen, S., and Vanderleyden, J. 2011. Auxin and plant-microbe interactions. Cold Spring Harbor perspectives in biology 3:a001438.
- St-Pierre, B., Vazquez-Flota, F.A., and De Luca, V. 1999. Multicellular compartmentation of Catharanthus roseus alkaloid biosynthesis predicts intercellular translocation of a pathway intermediate. The Plant Cell 11:887-900.
- Stopka, S.A., Agtuca, B.J., Koppenaal, D.W., Paša-Tolić, L., Stacey, G., Vertes, A., and Anderton, C.R. 2017. Laser-ablation electrospray ionization mass spectrometry with ion mobility separation reveals metabolites in the symbiotic interactions of soybean roots and rhizobia. The Plant Journal 91:340-354.
- Stopka, S.A., Samarah, L., Shaw, J.B., Liyu, A.V., Veličković, D., Agtuca, B.J., Kukolj, C., Koppenaal, D.W., Stacey, G., and Paša-Tolić, L. 2019. Ambient Metabolic Profiling and Imaging of Biological Samples with Ultrahigh Molecular Resolution using Laser Ablation Electrospray Ionization 21 Tesla FTICR Mass Spectrometry. Analytical chemistry.

**Agtuca** 

MPMI

Streeter, J., Lohnes, D., and Fioritto, R. 2001. Patterns of pinitol accumulation in soybean plants and relationships to drought tolerance. Plant, Cell & Environment 24:429-438.

- Streeter, J.G. 1980. Carbohydrates in soybean nodules: II. Distribution of compounds in seedlings during the onset of nitrogen fixation. Plant physiology 66:471-476.
- Streeter, J.G., and Bosler, M.E. 1976. Carbohydrates in soybean nodules: identification of compounds and possible relationships to nitrogen fixation. Plant Science Letters 7:321-329.
- Subramanian, S., Stacey, G., and Yu, O. 2007. Distinct, crucial roles of flavonoids during legume nodulation. Trends in plant science 12:282-285.
- Sutton, M.A., Oenema, O., Erisman, J.W., Leip, A., van Grinsven, H., and Winiwarter, W. 2011. Too much of a good thing. Nature 472:159.
- Tadra-Sfeir, M., Souza, E., Faoro, H., Müller-Santos, M., Baura, V., Tuleski, T., Rigo, L., Yates, M., Wassem, R., and Pedrosa, F. 2011. Naringenin regulates expression of genes involved in cell wall synthesis in Herbaspirillum seropedicae. Appl. Environ. Microbiol. 77:2180-2183.
- Tenenboim, H., and Brotman, Y. 2016. Omic relief for the biotically stressed: metabolomics of plant biotic interactions. Trends in plant science 21:781-791.
- Tilman, D., Balzer, C., Hill, J., and Befort, B.L. 2011. Global food demand and the sustainable intensification of agriculture. Proceedings of the National Academy of Sciences 108:20260-20264.
- Tiwari, R., Awasthi, A., Mall, M., Shukla, A.K., Srinivas, K.S., Syamasundar, K., and Kalra, A. 2013. Bacterial endophyte-mediated enhancement of in planta content of key terpenoid indole alkaloids and growth parameters of Catharanthus roseus. Industrial crops and products 43:306-310.
- Vacheron, J., Desbrosses, G., Bouffaud, M.-L., Touraine, B., Moënne-Loccoz, Y., Muller, D., Legendre, L., Wisniewski-Dyé, F., and Prigent-Combaret, C. 2013. Plant growth-promoting rhizobacteria and root system functioning. Frontiers in plant science 4:356.
- Van Moerkercke, A., Fabris, M., Pollier, J., Baart, G.J., Rombauts, S., Hasnain, G., Rischer, H., Memelink, J., Oksman-Caldentey, K.-M., and Goossens, A. 2013. CathaCyc, a metabolic pathway database built from Catharanthus roseus RNA-Seq data. Plant and cell physiology 54:673-685.
- Veličković, D., Agtuca, B.J., Stopka, S.A., Vertes, A., Koppenaal, D.W., Paša-Tolić, L., Stacey, G., and Anderton, C.R. 2018. Observed metabolic asymmetry within soybean root nodules reflects unexpected complexity in rhizobacteria-legume metabolite exchange. The ISME journal 12:2335.
- Verma, P., Mathur, A.K., Srivastava, A., and Mathur, A. 2012. Emerging trends in research on spatial and temporal organization of terpenoid indole alkaloid pathway in Catharanthus roseus: a literature update. Protoplasma 249:255-268.
- Wanek, W., and Richter, A. 1997. Biosynthesis and accumulation of D-ononitol in Vigna umbellata in response to drought stress. Physiologia Plantarum 101:416-424.
- Wasternack, C. 2007. Jasmonates: an update on biosynthesis, signal transduction and action in plant stress response, growth and development. Ann. Bot. 100:681-697.

MPMI

Wasternack, C., and Hause, B. 2013. Jasmonates: biosynthesis, perception, signal transduction and action in plant stress response, growth and development. An update to the 2007 review in Annals of Botany. Ann. Bot. 111:1021-1058.

- Webster, G., Jain, V., Davey, M., Gough, C., Vasse, J., Denarie, J., and Cocking, E. 1998. The flavonoid naringenin stimulates the intercellular colonization of wheat roots by Azorhizobium caulinodans. Plant, Cell & Environment 21:373-383.
- Westhoff, P. 2009. The economics of biological nitrogen fixation in the global economy. Nitrogen fixation in crop production. Agronomy Monograph 52:309-328.
- Widemann, E., Miesch, L., Lugan, R., Holder, E., Heinrich, C., Aubert, Y., Miesch, M., Pinot, F., and Heitz, T. 2013. The amidohydrolases IAR3 and ILL6 contribute to jasmonoyl-isoleucine hormone turnover and generate 12-hydroxyjasmonic acid upon wounding in Arabidopsis leaves. Journal of Biological Chemistry 288:31701-31714.
- Zivy, M., Wienkoop, S., Renaut, J., Pinheiro, C., Goulas, E., and Carpentier, S. 2015. The quest for tolerant varieties: the importance of integrating "omics" techniques to phenotyping. Frontiers in plant science 6:448.

## FIGURE LEGENDS

**Agtuca** 

Fig. 1 Schematic of experimental design. Three-day-old seedlings of *Setaria viridis* A10.1 were inoculated with either *H. seropedicae* SmR1 (fix\*) or SmR54 (fix\*), while the control (CTRL) plants were uninoculated. The plants grew for two weeks after inoculation under greenhouse conditions. The roots and leaves were harvested. Roots from plants that were inoculated with SmR1 or SmR54 were analyzed by fluorescence microscopy. The root area with the highest GFP expression, indicative of endophytic bacterial colonization, were cut into segments and used for analyses. The roots from uninoculated control plants were observed by microscopy and screening for GFP to check if there was any bacterial contamination, and then a comparable root segment was taken for analysis. Finally, the youngest, newly emerged sink leaf, the selected root segments, and the free-living bacterial cultures were analyzed by LAESI-MS using previously described methods (Stopka et al., 2017).

Fig. 2 Comparison of root segments from uninoculated (CTRL) plants in red and plants that were inoculated with either SmR1 (fix+) in green or SmR54 (fix-) in blue.

(a) Heat map of the significant metabolites that were abundant in each sample group. The red row z-score indicates the highest abundance, while the dark blue is the lowest abundance. Each row represents a metabolite, while the column characterizes the biological replicates from each sample group. (b) PLS-DA plot showing the covariance of all root sample groups. (c) Volcano plots presenting the number of spectral features that were statistically different with at least a fold change of 2 and a p-value < 0.05. The first plot shows the lower abundance in CTRL roots and the higher abundance in roots that were colonized by SmR1. The second plot represents the lower abundance in CTRL roots, while the higher abundance in SmR54 roots. The third plot represents the inoculated roots of SmR1 at lower abundance, while the SmR54 at higher abundance. (d) Box-and-whisker plots of four significant metabolites showing their relative abundances.

Fig. 3 Differences between spectra of uninoculated and inoculated plants, comparing to the root and leaf samples. PLS-DA scores plot showing contrast between the spectra of leaf and root samples. Root segment spectra of CTRL are in red, SmR1 are in green, and SmR54 are in blue. Leaf sample spectra of CTRL are in yellow, SmR1 are in light gray, and SmR54 are in dark gray.

MPMI

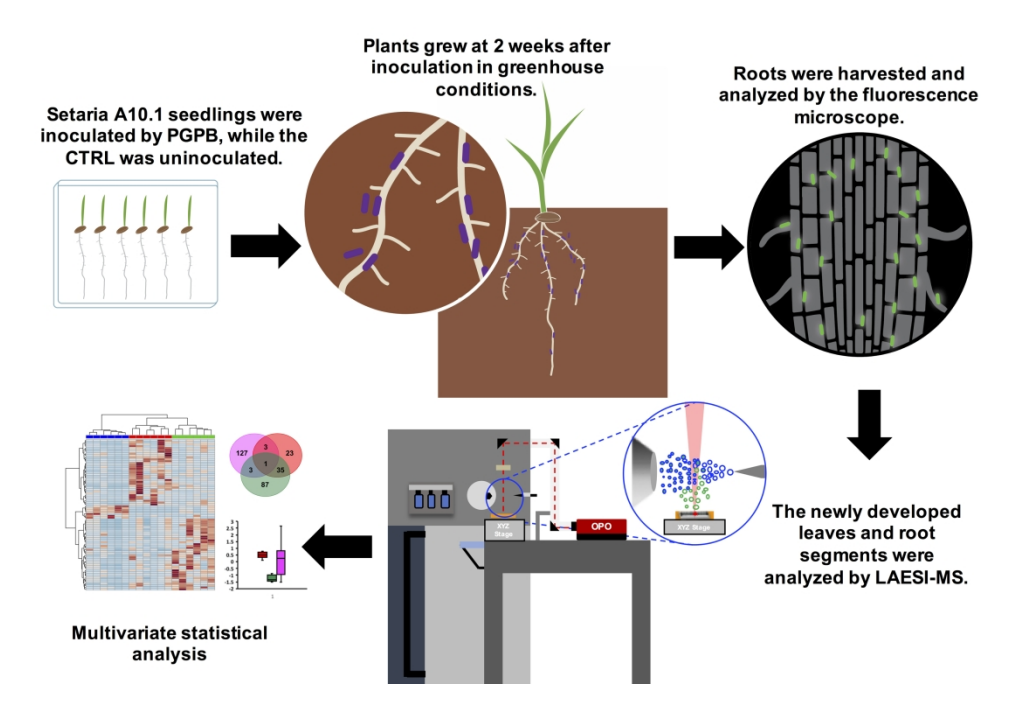
Fig. 4 Metabolic pathways significantly impacted by infection with SmR1 H. seropedicae (fix<sup>+</sup>; green) or with SmR54 H. seropedicae (fix<sup>-</sup>; blue). All the identified metabolites with a fold change > 2 and a p-value < 0.05 were used for the enrichment analysis using the MetaboAnalyst 4.0 web resource using the rice metabolite library as reference. These pathways highlight the importance of symbiosis, BNF, growth promotion, and metabolism. The pathway analyses had a range of p values  $10^{-6}$ 

## **TABLE TITLES**

3×10<sup>-1</sup>.

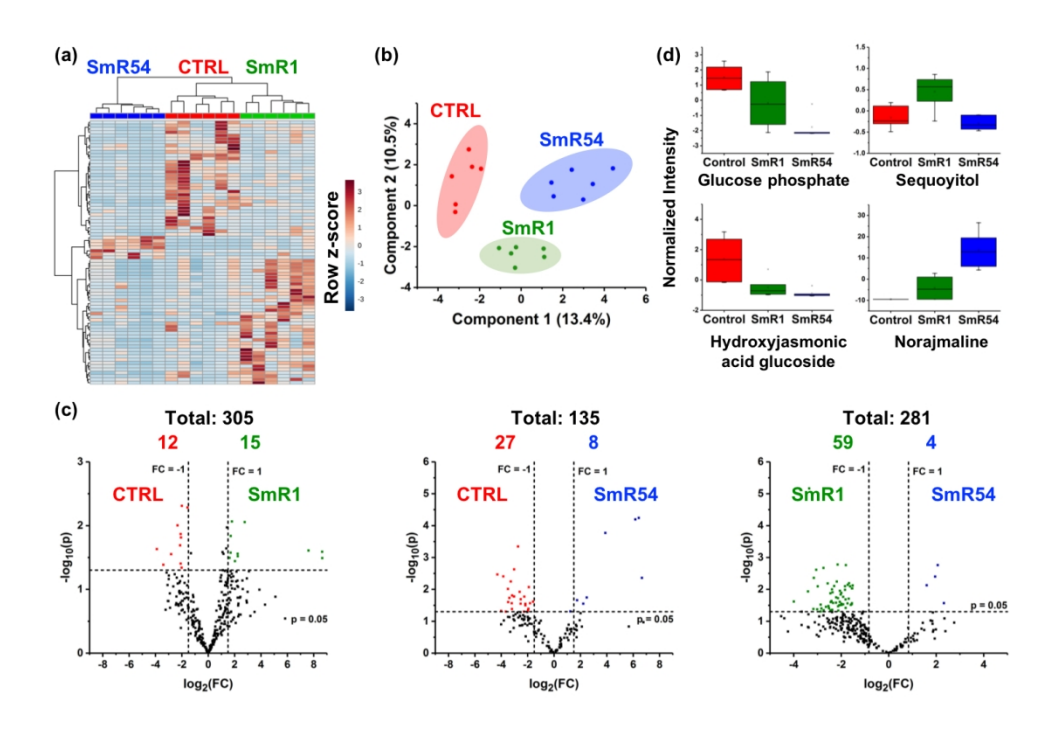
**Agtuca** 

Table 1 List of identified metabolites and pathways affected in *Setaria viridis* roots infected with either SmR1 or SmR54. The uninoculated (CTRL) plants were also analyzed for comparison. These metabolites had a significant fold change of at least 2 and p-value of < 0.05 shown in bold. The positive fold change is the up-regulation number, while the negative fold change is the down-regulation in abundance.



**Fig. 1. Schematic of experimental design.** Three-day-old seedlings of *Setaria viridis* A10.1 were inoculated with either *H. seropedicae* SmR1 (fix<sup>+</sup>) or SmR54 (fix<sup>-</sup>), while the control (CTRL) plants were uninoculated. The plants grew for two weeks after inoculation under greenhouse conditions. The roots and leaves were harvested. Roots from plants that were inoculated with SmR1 or SmR54 were analyzed by fluorescence microscopy. The root areas with the highest GFP expression, indicative of endophytic bacterial colonization, were cut into segments and used for analyses. The roots from uninoculated control plants were observed by microscopy and screening for GFP to check if there was any bacterial contamination, and then comparable root segments was taken for analysis. Finally, the youngest, newly emerged sink leaf, the selected root segments, and the free-living bacterial cultures were analyzed by LAESI-MS using previously described methods (Stopka et al. (2017)).

267x175mm (300 x 300 DPI)



**Fig. 2.** Comparison of root segments from uninoculated (CTRL) plants in red and plants that were inoculated with either SmR1 (fix<sup>+</sup>) in green or SmR54 (fix<sup>-</sup>) in blue. (a) Heat map of the significant metabolites that were abundant in each sample group. The red row z-score indicates the highest abundance, while the dark blue is the lowest abundance. Each row represents a metabolite, while the column characterizes the biological replicates from each sample group. (b) PLS-DA plot showing the covariance of all root sample groups. (c) Volcano plots presenting the number of spectral features that were statistically different with at least a fold change of 2 and a p-value < 0.05. The first plot shows the lower abundance in CTRL roots and the higher abundance in roots that were colonized by SmR1. The second plot represents the lower abundance in CTRL roots, while the higher abundance in SmR54 roots. The third plot represents the inoculated roots of SmR1 at lower abundance, while the SmR54 at higher abundance. (d) Box-and-whisker plots of four significant metabolites showing their relative abundances.

257x180mm (150 x 150 DPI)

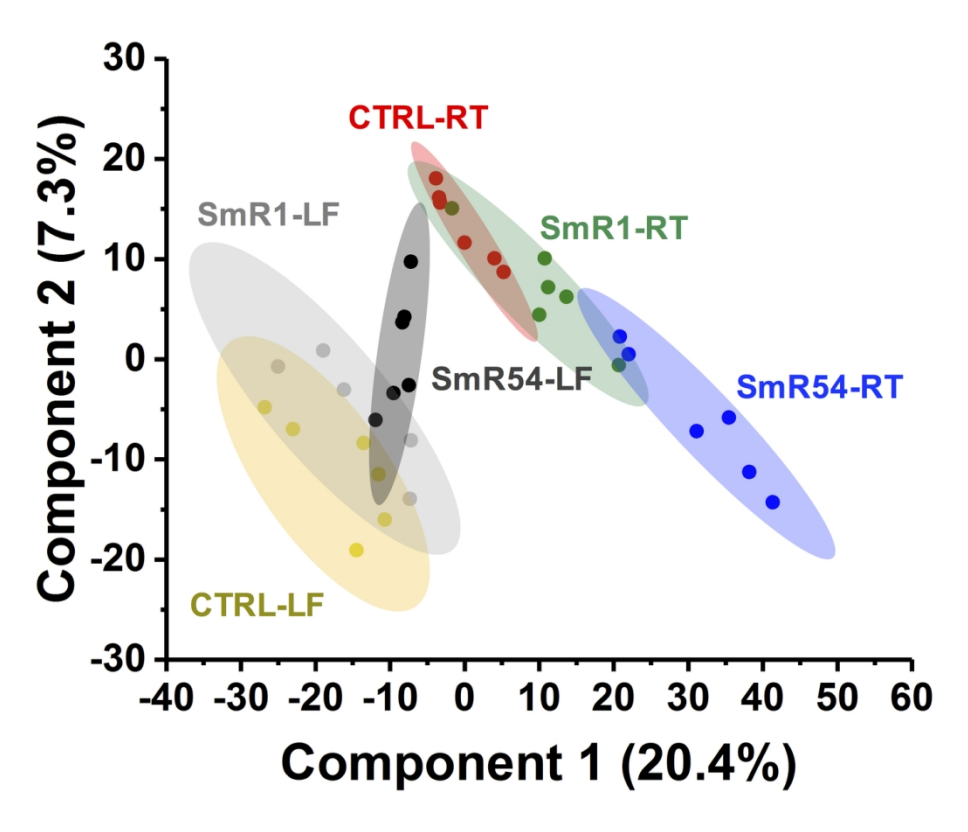


**Fig. 3. Differences between spectra of uninoculated and inoculated plants, comparing the root and leaf samples.** PLS-DA scores plot showing contrast between the spectra of leaf and root samples. Root segment spectra of CTRL are in red, SmR1 are in green, and SmR54 are in blue. Leaf sample spectra of CTRL are in yellow, SmR1 are in light gray, and SmR54 are in dark gray.

131x109mm (300 x 300 DPI)

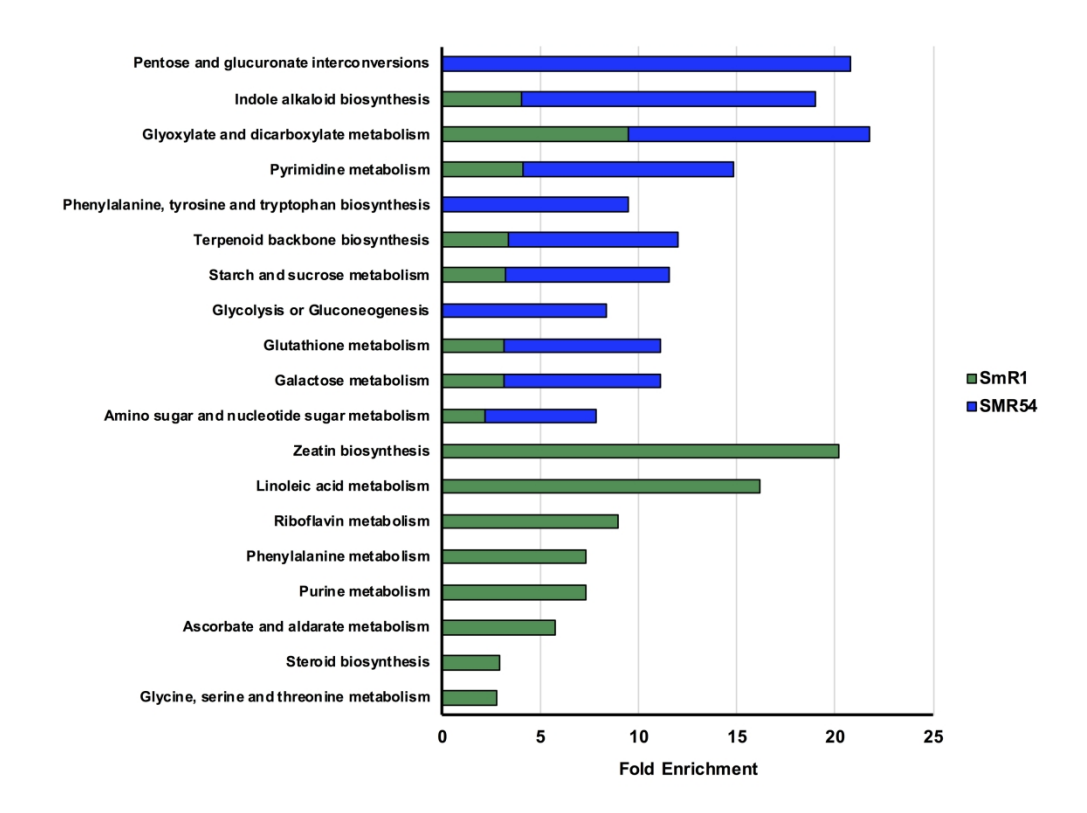


Fig. 4. Metabolic pathways significantly impacted by infection with SmR1 H. seropedicae (fix<sup>+</sup>; green) or with SmR54 H. seropedicae (fix<sup>-</sup>; blue). All the identified metabolites with a fold change > 2 and a p-value < 0.05 were used for the enrichment analysis using the MetaboAnalyst 4.0 web resource using the rice metabolite library as reference. These pathways highlight the importance of symbiosis, BNF, growth promotion, and metabolism. The pathway analyses had a range of p values  $8 \times 10^{-7} .$ 

241x182mm (300 x 300 DPI)

Table 1. List of identified metabolites and pathways affected in *Setaria viridis* roots infected with either SmR1 or SmR54. The uninoculated (CTRL) plants were also analyzed for comparison. These metabolites had a significant fold change of at least 2 and p-value of < 0.05 shown in bold. The positive fold change is the up-regulation number, while the negative fold change is the down-regulation in abundance.

				Log <sub>2</sub> (FC)	
Pathways	Metabolites	KEGG ID	SmR1 vs. CTRL	SmR54 vs. CTRL	SmR54 vs. SmR1
	Methylpyranosyl glucoside <sup>a</sup>		5.10	6.67**	2.33*
	Hydroxybutyrate glucoside <sup>a</sup>		-0.05	-2.24	-2.40*
	Trihydroxyflavonea	C06563	-1.63	-3.48	-2.86*
	Dimethoxy-flavone	C11620	1.67	-0.97	-3.34**
	Tetramethoxyflava none <sup>a</sup>	C14472	1.50		-2.22*
-, .,	Acetyl- prenylphenol glucoside <sup>a</sup>	C04608	1.79	-1.88	-2.51*
Flavonoid Biosynthesis	Hydroxyflavanone glucoside <sup>a</sup>	C16989	1.62*	1.76*	-1.44
	Dihydrochalcone glucoside	C01604	-0.52		-2.05*
	Dihydroxy methoxyflavone glucoside <sup>a</sup>	C10381	0.16		-2.29*
	Hydroxy dimethoxyflavone glucoside <sup>a</sup>		0.69		-2.13*
	Dihydroxyisoflavon e malonyl glucoside <sup>a</sup>	C16191	2.24*		-1.62

	Trihydroxy trimethoxyflavone glucoside		-0.69	-1.90*	-2.02*
	Trihydroxy- tetramethoxyflavo ne glucoside		-1.50	-3.18*	
	Glucose <sup>a</sup>	C00031	-0.48	-1.81*	-1.53*
Starch and Sucrose Metabolism	Glucose Phosphate <sup>a</sup>	C00103	-1.30*	-3.02**	-1.65
	Dissacharidea	C00089	-2.06*	-3.84**	-1.97
Cysteine and	Sulfolactatea	C11537	-2.12*	-3.28*	-0.75
methionine metabolism	Gutathionea	C00051	-2.01*	-3.20*	
Pyrimidine	UDPa	C00015	-1.50	-2.52*	
metabolism	UMPa	C00105	0.38	-2.56	-1.73*
Indole alkaloid	Norajmaline	C11810	8.65*	6.17**	2.07**
biosynthesis	Ajmalineª	C06542	8.65*	6.43**	1.60*
Phenylpropanoid	Sinapoylglucosea	C01175	-1.15	-3.03*	-2.36*
biosynthesis	Pimpinellin <sup>a</sup>	C09285	-2.08*	-3.49*	
Fatty acid	Heptose phosphate <sup>a</sup>	C07836	-0.24		-1.51*
biosynthesis	Hydroxyjasmonic acid glucoside <sup>a</sup>	C08558	-2.08*	-3.18*	-1.68
Pentose and					
glucuronate interconversions	Gulonatea	C00800	0.11	-1.94*	-2.22
Naphthalene degradation	Dihydroibenzothio phene	C14092	0.50	-1.59*	-1.99
Puromycin biosynthesis	Puromycin aminonucleoside	C01610	3.09*	3.89*	1.96**
Salicylate degradation	Dihydroxybenzoat e glucoside <sup>a</sup>	C00628	0.13	-2.25*	-3.05**
Aminobenzoate degradation	Dehydrodivanillate a	C18347	-2.00**	-2.60*	-1.70

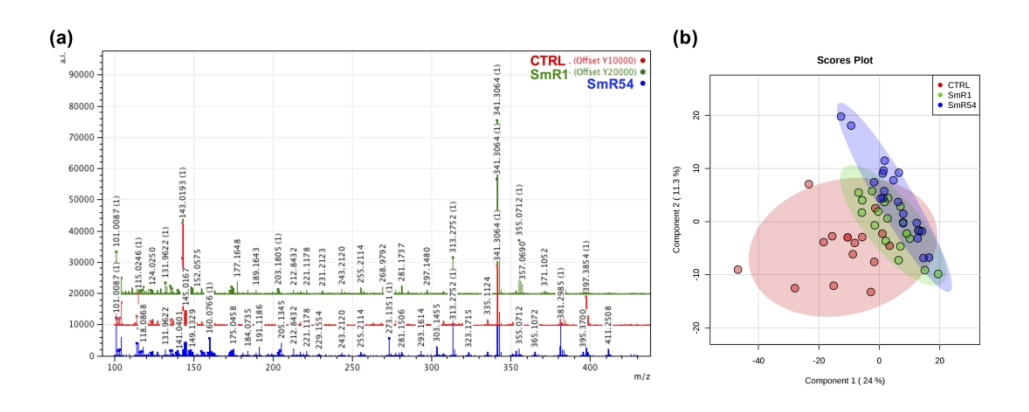
Agtuca

MPMI

Dyrunyata					
Pyruvate metabolism	Lactoylglutathione	C03451	-1.13	-3.02*	-1.68
	Thiolutin/ methylmalate		-0.41	-2.76	-2.56*
	Sequoyitola	C03365	1.43*		-2.15**
Miscellaneous	Methylbutanoylapi osylhexose <sup>a</sup>	C11916	1.12*		-1.84*
	Bis(glycerophosph oglycerol)	C03274	-0.65	-2.27*	-1.96

<sup>\*</sup>P < 0.05 and \*\*P < 0.005

<sup>&</sup>lt;sup>a</sup> Metabolites assigned by in-house reference standard MS/MS performed under identical conditions.



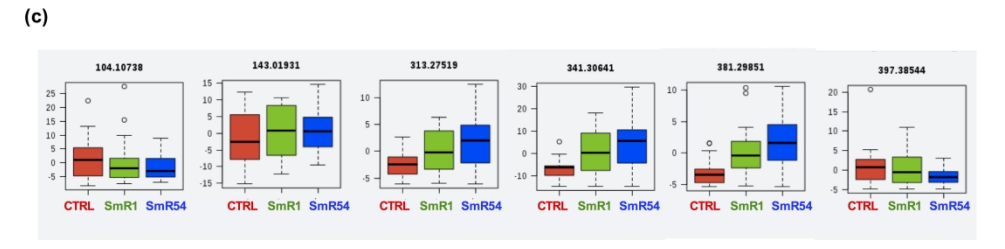


**Fig. S1. Bulk analyses of Setaria roots segments.** (a) Mass spectra of root segments: uninoculated plants (CTRL; in red) and plants that were inoculated by either *H. seropedicae* SmR1 (fix<sup>+</sup>; in green) or SmR54 (fix<sup>-</sup>; in blue). (b) A PLS-DA scores plot showing no separation for the spectra of the three different root segment sample types. (c) Box-and-whisker plots for unidentified compounds that display no differences in their abundances.

259x167mm (300 x 300 DPI)

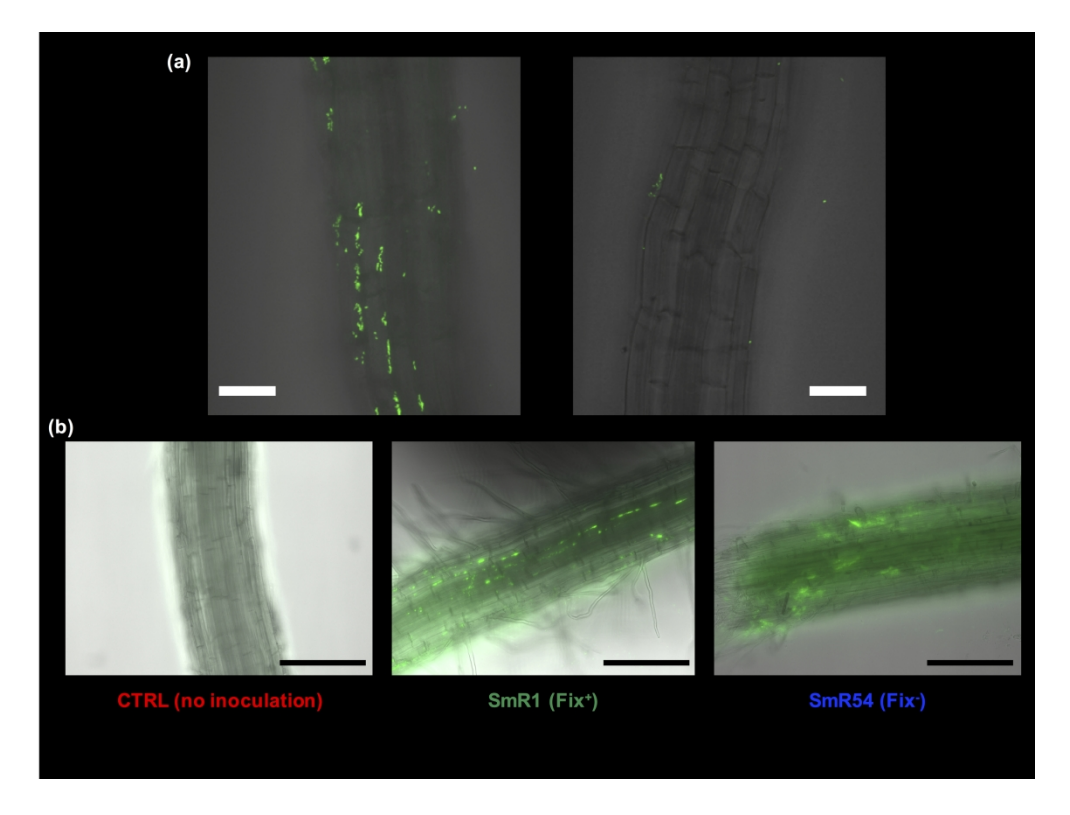


**Fig. S2. Microscopy images of bacterial colonization.** (a) Images by confocal microscopy: right image demonstrates a root segment with colonization endophytically and epiphytically by *H. seropedicae* SmR1, and left image displays a root segment with colonization epiphytically by *H. seropedicae* SmR1. (b) Images by fluorescence microscopy. Left image exemplifies that there was no bacterial colonization in the uninoculated roots. Middle image represents colonization by SmR1 on the roots, whereas right image shows SmR54 colonization. These roots were cut into segments for LAESI-MS analyses. White and black scale bars = 50 μm

255x190mm (300 x 300 DPI)

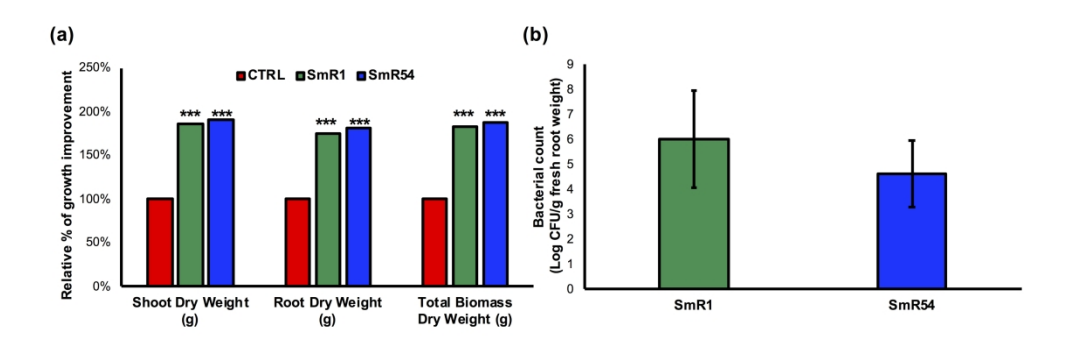


**Fig. S3.** Growth promotion of Setaria viridis A10.1 inoculated by either *H. seropedicae* SmR1 (fix<sup>+</sup>) or SmR54 (fix<sup>-</sup>). (a) Plants were grown with no addition of nitrate and harvested at 3 weeks after inoculation. The data represents % growth changes in inoculated plants compared to the uninoculated plants (n = 30). The dry weight (g) of roots and leaves and total biomass were analyzed. Asterisks represent the statistically significant differences as determined by t-tests; \*\*\*, p-value <0.001. (b) The total root colonization by SmR1 and SmR54 in Setaria roots at 2 weeks after inoculation. Bars represent ± SD.

254x90mm (300 x 300 DPI)

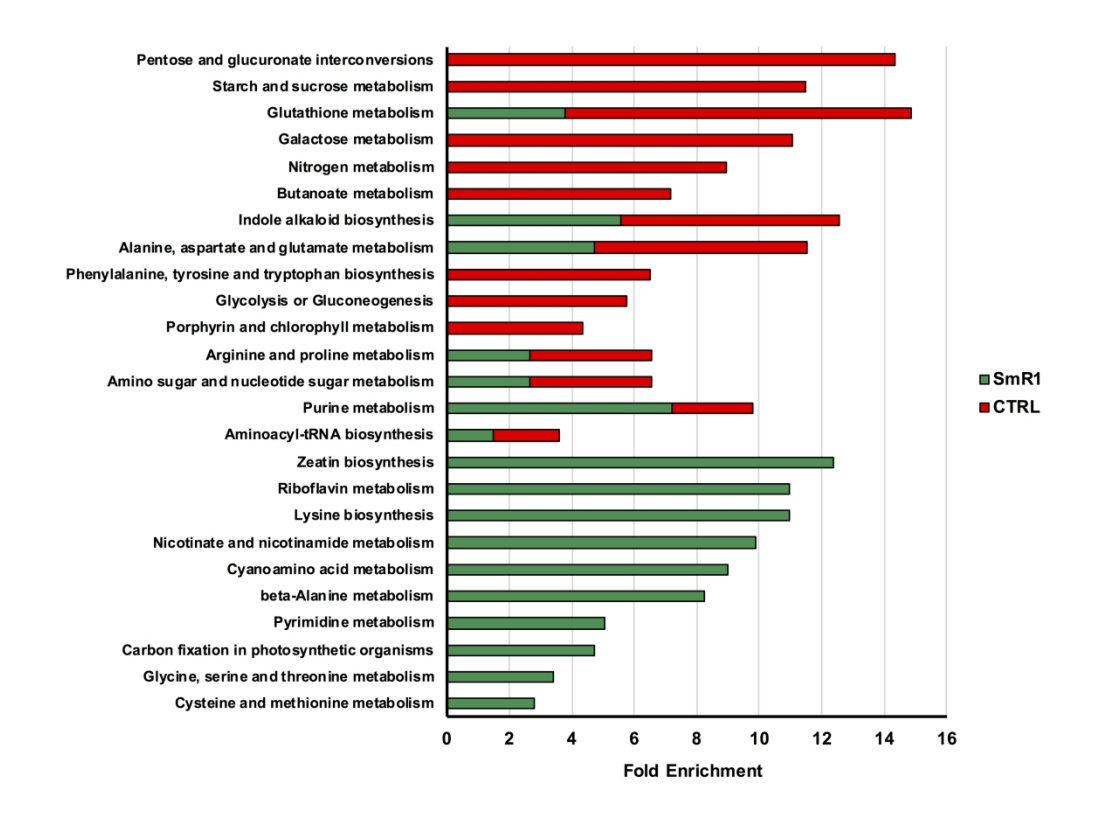


Fig. S4. Enriched pathways detected when comparing plants inoculated by SmR1 (fix<sup>+</sup>; green) versus the uninoculated plants (CTRL; red). These pathways highlight functions of importance to biological nitrogen fixation, growth promotion, symbiosis, and metabolism. All the identified metabolites were used for enrichment analyses. Pathway analysis showed a range of p-values  $4 \times 10^{-4} .$ 

240x182mm (300 x 300 DPI)

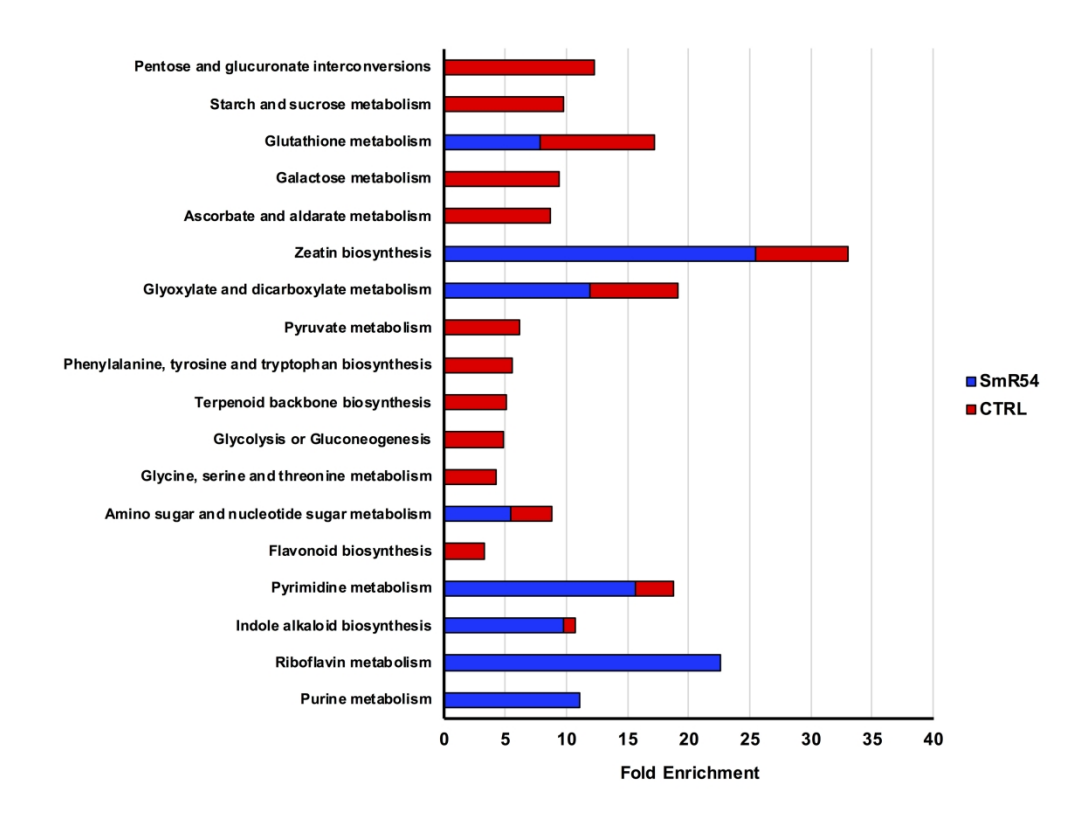


Fig. S5. Pathways enriched for symbiosis and metabolism compared for uninoculated plants (CTRL; red) and inoculated plants of SmR54 ( $fix^-$ ; blue). All the identified metabolites were used for enrichment analyses. Pathway analysis showed a range of p-values  $4 \times 10^{-3} < p$ -value  $< 4 \times 10^{-1}$ .

240x182mm (300 x 300 DPI)

Table S1. Identified metabolites and pathways abundant in *Setaria viridis* youngest newly emerged sink leaf with roots either infected by SmR1 or SmR54, or the uninoculated plants (CTRL). These metabolites had a significant fold change of at least 2 and a p-value of < 0.05 shown in bold. The positive fold change is the up-regulation number, while the negative fold change is the down-regulation in abundance.

				Log <sub>2</sub> (FC)	
Pathways	Metabolites	KEGG ID	SmR1 vs. CTRL	SmR54 vs. CTRL	SmR54 vs. SMR1
	Glyoxylate	C00048	-2.48*	-0.33	1.92*
	Glutamatea	C00025	-3.08*	-0.98	2.11
Purine metabolism	Guanosinea	C00387	-2.56*	-0.36	2.43*
	Adenosine phosphate	C00020	2.31**	2.13*	0.77
	GMPa	C00144	0.83	1.97*	2.77
	PC (33:2) <sup>a</sup>	<u></u>	-4.58	-0.41	4.16*
	PG (34:3) <sup>a</sup>		-3.32**	0.08	1.39
Glycerophospholipid metabolism	PC (33:2) <sup>a</sup>		-3.49*	-0.05	
	PI (34:3) <sup>a</sup>		-4.58*	0.63	1.33
	PI (34:2) <sup>a</sup>		-3.99*	-0.01	2.34
	Luteolin glucuronide	C03515	0.29	1.57*	1.61
	Quercetagetin glucoside <sup>a</sup>	C05623	2.05**		
Flavonoid biosynthesis	Kaempferol diglucoside <sup>a</sup>	C12667	-3.19*	-1.32	1.97
2.00,	Kaempferide triglycoside		-3.64	0.56	4.78*
	Tetramethoxyfl avone glucoside <sup>a</sup>			1.96*	0.62

**MPMI** 

**Agtuca** 

_	Sucrose <sup>a</sup>	C00089	0.67	2.28*	1.72*
	Ferulyl glucose	C17759	-2.76	0.12	2.77*
Starch and sucrose metabolism	Hexose phosphate <sup>a</sup>	C00668	-0.3	1.16	1.56*
	Monosaccharid e <sup>a</sup>	C00181	-2.33*	-1.23*	0.39
	Maleatea	C01384	-1.85*	0.12	2.05*
Butanoate metabolism	Malate <sup>a</sup>	C00497	-1.83*	0.14	2.02*
	Hexylmalate	C17227	0.72	1.40*	1.02
Plant hormone	Indole-3-acetic acid	C00954	1.59*		-0.81
signal transduction	Hydroxyjasmo nic acid glucoside <sup>a</sup>	C08558	0.84	2.76*	1.37
	Lactaldehyde	C00424	2.27*		-1.15
Pyruvate Metabolism	Lactoylglutathi one	C03451	2.68*	1.93*	-0.4
Aminobenzoate	Nitrocatechol	C02235	-0.47	0.35	-1.73*
degradation	Dehydrodivanil late <sup>a</sup>	C18347	0.63	2.57*	4.49*
Phenylpropanoid	Chavicol	C16930	-1.73*	-0.39	0.69
biosynthesis	Pimpinellina	C09285	0.8	-1.03*	-1.81
Amino acid metabolism	Pyrroline carboxylate	C04281	-2.59*	1.54*	2.18*
metabonam	Tryptophana	C00078	0.14	-1.64	-2.08*
Polycyclic aromatic hydrocarbon degradation	2-oxobut-3- enoate	C16149	2.22*	-1.70*	-0.01
Citrate cycle	Citratea	C00158	1.39*	-2.23	-1.77*
Puromycin biosynthesis	Puromycin aminonucleosi de	C01610		1.89*	2.34*
Folate biosynthesis	Amino hydroxy dihydropteridin	C04895		2.58*	1.8

Agtuca

MPMI

	Riboflavin cyclic phosphate	C16071	1.44	1.65*	0.29
	Diapolycopene dioate		-1.94*	-1.35*	-0.22
Miscellaneous	Dalnigrein glucopyranosid e			2.13*	2.65*
	Benzaldehyde		-0.87	-1.89*	-1.08
	Methyl erythritol phosphate <sup>a</sup>		2.70*	1.24	-1.43

<sup>\*</sup>P < 0.05 and \*\*P < 0.005

<sup>&</sup>lt;sup>a</sup> Metabolites assigned by in-house reference standard MS/MS performed under identical conditions.

Table S2. Identified metabolites and pathways that were affected between *Setaria viridis* inoculated with SmR1 and CTRL plants that were not infected. These metabolites were significant by ANOVA with a f-value range of 3 to 130. The samples that were analyze were SmR1-RT, SmR1-LF, SmR1-Bact, CTRL-RT, and CTRL-LF.

Sample	Pathways	Metabolites	KEGG ID	f.value	Fisher's LSD
		Hydroxy dimethoxyflavone glucoside <sup>a</sup>		8.19*	SmR1-RT > CTRL-RT; SmR1- RT > CTRL-LF; SmR1-RT > SmR1-Bact; SmR1-RT > SmR1-LF
		Dihydroxyisoflavone malonyl glucoside <sup>a</sup>	C16191	5.31*	SmR1-RT > CTRL-RT; SmR1- RT > CTRL-LF; SmR1-RT > SmR1-Bact; SmR1-RT > SmR1-LF
		Coumesterola	C10205	5.16*	SmR1-RT > CTRL-RT; SmR1- RT > CTRL-LF; SmR1-RT > SmR1-Bact; SmR1-RT > SmR1-LF
		Dihydroxy methoxyflavone glucoside <sup>a</sup>	C10381	5.07*	SmR1-RT > CTRL-RT; SmR1- RT > CTRL-LF; SmR1-RT > SmR1-Bact; SmR1-RT > SmR1-LF
SmR1-RT	Flavonoid Biosynthesis	Dimethoxy-flavone	C10029	4.84*	SmR1-RT > CTRL-RT; SmR1- RT > CTRL-LF; SmR1-RT > SmR1-Bact; SmR1-RT > SmR1-LF
ω		Tetrahydroxyflavano ne glucoside <sup>a</sup>	C16408	4.62*	SmR1-RT > CTRL-RT; SmR1- RT > CTRL-LF; SmR1-RT > SmR1-Bact; SmR1-RT > SmR1-LF
		Acetyl-prenylphenol glucoside	C04608	4.43*	SmR1-RT > CTRL-RT; SmR1- RT > CTRL-LF; SmR1-RT > SmR1-Bact; SmR1-RT > SmR1-LF
		Tetramethoxyflavan one <sup>a</sup>	C14472	3.99*	SmR1-RT > CTRL-RT; SmR1- RT > CTRL-LF; SmR1-RT > SmR1-Bact; SmR1-RT > SmR1-LF
		Trihydroxyflavonea	C06563	3.94*	SmR1-RT > CTRL-LF; SmR1- RT > SmR1-Bact; SmR1-RT > SmR1-LF
	Indole	Ajmaline <sup>a</sup>	C06542	6.72*	SmR1-RT > CTRL-RT; SmR1- RT > CTRL-LF; SmR1-RT >

	alkaloid biosynthesis				SmR1-Bact; SmR1-RT > SmR1-LF
		Norajmaline	C11810	5.90*	SmR1-RT > CTRL-RT; SmR1- RT > CTRL-LF; SmR1-RT > SmR1-Bact; SmR1-RT > SmR1-LF
	Puromycin biosynthesis	Puromycin aminonucleoside	C01610	5.56*	SmR1-RT > CTRL-RT; SmR1- RT > CTRL-LF; SmR1-RT > SmR1-Bact; SmR1-RT > SmR1-LF
	Starch and sucrose metabolism	Methylbutanoylapios ylhexose <sup>a</sup>	C11916	4.81*	SmR1-RT > CTRL-RT; SmR1- RT > CTRL-LF; SmR1-RT > SmR1-Bact; SmR1-RT > SmR1-LF
	Miscellaneou	Sulfolactaldehyde	C20798	15.89*	SmR1-RT > CTRL-RT; CTRL- RT > SmR1-Bact; CTRL-RT > SmR1-LF; SmR1-RT > CTRL- LF; SmR1-RT > SmR1-Bact; SmR1-RT > SmR1-LF
	S	Sequoyitol <sup>a</sup>	C03365	10.96*	SmR1-RT > CTRL-RT; SmR1- RT > CTRL-LF; SmR1-RT > SmR1-Bact; SmR1-RT > SmR1-LF
년 -	Amino acid	Citrate <sup>a</sup>	C00158	5.08*	SmR1-LF > CTRL-RT; CTRL- LF > SmR1-Bact; SmR1-LF > SmR1-RT; SmR1-LF > SmR1- Bact
SmR1-LF	metabolism	Aspartic acid <sup>a</sup>	C00049	5.01*	SmR1-LF > CTRL-RT; SmR1- LF > CTRL-LF; SmR1-LF > SmR1-RT; SmR1-LF > SmR1- Bact
		Sulfur dioxide	C09306	125.39*	SmR1-Bact > CTRL-RT; SmR1- Bact > CTRL-LF; SmR1-Bact > SmR1-RT; SmR1-Bact > SmR1-LF
Bact	Amino acid metabolism	Dihydroxybenzoate glucoside <sup>a</sup>	C00628	9.39*	SmR1-Bact > CTRL-RT; SmR1- Bact > CTRL-LF; SmR1-Bact > SmR1-RT; SmR1-Bact > SmR1-LF
SmR1-Bact		Glutathione <sup>a</sup>	C00051	6.59*	SmR1-Bact > CTRL-RT; SmR1- Bact > CTRL-LF; SmR1-Bact > SmR1-RT; SmR1-Bact > SmR1-LF
	Calcium signaling pathway	Cyclic-ADP ribose <sup>a</sup>	C13050	130.25*	SmR1-Bact > CTRL-RT; SmR1- Bact > CTRL-LF; SmR1-Bact > SmR1-RT; SmR1-Bact > SmR1-LF

Flavonoid biosynthesis	Dihydroxyflavone glucoside <sup>a</sup>	C10216	29.61*	SmR1-Bact > CTRL-RT; SmR1- Bact > CTRL-LF; SmR1-Bact > SmR1-RT; SmR1-Bact > SmR1-LF
	Urateª	C00366	73.41*	SmR1-Bact > CTRL-RT; SmR1- Bact > CTRL-LF; SmR1-Bact > SmR1-RT; SmR1-Bact > SmR1-LF
	Adenine <sup>a</sup>	C00147	56.62*	SmR1-Bact > CTRL-RT; SmR1- Bact > CTRL-LF; SmR1-Bact > SmR1-RT; SmR1-Bact > SmR1-LF
Purine	AMP <sup>a</sup>	C00020	47.96*	SmR1-Bact > CTRL-RT; SmR1- Bact > CTRL-LF; SmR1-Bact > SmR1-RT; SmR1-Bact > SmR1-LF
metabolism	Guanosine phosphate <sup>a</sup>	C06193	25.30*	SmR1-Bact > CTRL-RT; SmR1- Bact > CTRL-LF; SmR1-Bact > SmR1-RT; SmR1-Bact > SmR1-LF
	Guanosine	C00387	11.56*	SmR1-Bact > CTRL-RT; SmR1- Bact > CTRL-LF; SmR1-Bact > SmR1-RT; SmR1-Bact > SmR1-LF
	Adenosine Diphosphate <sup>a</sup>	C00008	10.33*	SmR1-Bact > CTRL-RT; SmR1- Bact > CTRL-LF; SmR1-Bact > SmR1-RT; SmR1-Bact > SmR1-LF
	UDP <sup>a</sup>	C00015	19.86*	SmR1-Bact > CTRL-RT; SmR1- Bact > CTRL-LF; SmR1-Bact > SmR1-RT; SmR1-Bact > SmR1-LF
Pyrimidine metabolism	CMP <sup>a</sup>	C00055	15.79*	SmR1-Bact > CTRL-RT; SmR1- Bact > CTRL-LF; SmR1-Bact > SmR1-RT; SmR1-Bact > SmR1-LF
	UMP <sup>a</sup>	C00105	4.16*	SmR1-Bact > CTRL-RT; SmR1- Bact > CTRL-LF; SmR1-Bact > SmR1-RT; SmR1-Bact > SmR1-LF
Riboflavin metabolism	Amino (ribitylamino) uracil	C04732	52.02*	SmR1-Bact > CTRL-RT; SmR1- Bact > CTRL-LF; SmR1-Bact > SmR1-RT; SmR1-Bact > SmR1-LF
Starch and sucrose metabolism	N-Acetyl- glucosamine phosphate	C00357	19.62*	SmR1-Bact > CTRL-RT; SmR1- Bact > CTRL-LF; SmR1-Bact > SmR1-RT; SmR1-Bact > SmR1-LF

		dTDP-hexose	C00842	4.24*	SmR1-Bact > CTRL-LF; SmR1- Bact > SmR1-RT; SmR1-Bact > SmR1-LF
		Acetyl dihexose <sup>a</sup>		75.81*	SmR1-Bact > CTRL-RT; SmR1- Bact > CTRL-LF; SmR1-Bact > SmR1-RT; SmR1-Bact > SmR1-LF
	Miscellaneou s	Riboflavin cyclic phosphate	C16071	57.77*	SmR1-Bact > CTRL-RT; SmR1- Bact > CTRL-LF; SmR1-Bact > SmR1-RT; SmR1-Bact > SmR1-LF
		Metaphosphoric acid	C02466	4.67*	SmR1-Bact > CTRL-RT; SmR1- Bact > CTRL-LF; SmR1-Bact > SmR1-RT; SmR1-Bact > SmR1-LF
	Amino acid metabolism	Sulfolactate/phosph olactate <sup>a</sup>	C11537	4.13*	CTRL-RT > SmR1-RT; CTRL- RT > SmR1-Bact; CTRL-RT > SmR1-LF
	Aminobenzoa te degradation	Dehydrodivanillatea	C18347	9.20*	CTRL-RT > CTRL-LF; CTRL- RT > SmR1-RT; CTRL-RT > SmR1-Bact; CTRL-RT > SmR1- LF; CTRL-LF > SmR1-Bact; SmR1-LF > SmR1-Bact
	Butanoate metabolism	Maleate <sup>a</sup>	C01384	4.38*	CTRL-RT > SmR1-Bact; CTRL- LF > SmR1-Bact; CTRL-LF > SmR1-LF; SmR1-RT > SmR1- Bact
L-RT		Luteolin glucuronide	C03515	7.31*	CTRL-RT > CTRL-LF; CTRL- RT > SmR1-RT; CTRL-RT > SmR1-LF; SmR1-Bact > CTRL- LF; SmR1-Bact > SmR1-RT; SmR1-Bact > SmR1-LF
CTRL-RT	Flavonoid biosynthesis	Hydroxyjasmonic acid glucoside <sup>a</sup>	C08558	6.73*	CTRL-RT > CTRL-LF; CTRL- RT > SmR1-RT; CTRL-RT > SmR1-Bact; CTRL-RT > SmR1- LF
		Quercetagetin glucoside <sup>a</sup>	C05623	3.69*	CTRL-RT > CTRL-LF; CTRL- RT > SmR1-RT; CTRL-RT > SmR1-Bact; CTRL-RT > SmR1- LF
	Phenylpropa noid Biosynthesis	Pimpinellin <sup>a</sup>	C09285	5.95*	CTRL-RT > SmR1-RT; CTRL- RT > SmR1-Bact; CTRL-RT > SmR1-LF; CTRL-LF > SmR1- RT; CTRL-LF > SmR1-Bact
		Sinapoylglucose <sup>a</sup>	C01175	5.71*	CTRL-RT > CTRL-LF; CTRL- RT > SmR1-RT; CTRL-RT > SmR1-Bact; CTRL-RT > SmR1- LF

	Purine metabolism	Pentose phosphate <sup>a</sup>		4.09*	CTRL-RT > SmR1-Bact; CTRL- LF > SmR1-RT; CTRL-LF > SmR1-Bact; SmR1-LF > SmR1- Bact
		Sucrose <sup>a</sup>	C00089	8.00*	CTRL-RT > CTRL-LF; CTRL- RT > SmR1-RT; CTRL-RT > SmR1-Bact; CTRL-RT > SmR1- LF
	Starch and	Trisaccharide		6.77*	CTRL-RT > CTRL-LF; CTRL- RT > SmR1-RT; CTRL-RT > SmR1-Bact; CTRL-RT > SmR1- LF
	sucrose metabolism	Glucose phosphate <sup>a</sup>	C00103	5.35*	CTRL-RT > CTRL-LF; CTRL- RT > SmR1-RT; CTRL-RT > SmR1-Bact; CTRL-RT > SmR1- LF
		Glucose <sup>a</sup>	C00031	3.75*	CTRL-RT > SmR1-Bact; CTRL- LF > SmR1-Bact; SmR1-RT > SmR1-Bact; SmR1-LF > SmR1- Bact
	Miscellaneou s	Galactopinitol <sup>a</sup>	4	4.78*	CTRL-RT > CTRL-LF; CTRL- RT > SmR1-RT; CTRL-RT > SmR1-Bact; CTRL-RT > SmR1- LF
	Amino acid	Shitimic acida	C00493	7.73*	CTRL-LF > CTRL-RT; CTRL-LF > SmR1-RT; CTRL-LF > SmR1- Bact; CTRL-LF > SmR1-LF; SmR1-LF > SmR1-Bact
	metabolism	Glutamate <sup>a</sup>	C00025	6.33*	CTRL-LF > CTRL-RT; CTRL-LF > SmR1-RT; CTRL-LF > SmR1- Bact; CTRL-LF > SmR1-LF
	Butanoate metabolism	Malate <sup>a</sup>	C00497	5.60*	CTRL-LF > CTRL-RT; CTRL-LF > SmR1-RT; CTRL-LF > SmR1- Bact; CTRL-LF > SmR1-LF
CTRL-LF	Polycyclic aromatic hydrocarbon degradation	2-oxobut-3-enoate	C16149	6.53*	CTRL-LF > CTRL-RT; CTRL-LF > SmR1-RT; CTRL-LF > SmR1- Bact; CTRL-LF > SmR1-LF
		Oxoalate	C00209	8.51*	CTRL-LF > CTRL-RT; CTRL-LF > SmR1-RT; CTRL-LF > SmR1- Bact; CTRL-LF > SmR1-LF
	Purine metabolism	GMP <sup>a</sup>	C00144	5.43*	CTRL-LF > CTRL-RT; SmR1- LF > CTRL-RT; CTRL-LF > SmR1-RT; CTRL-LF > SmR1- Bact; SmR1-LF > SmR1-RT; SmR1-LF > SmR1-Bact

MPMI

SmR1-LF > SmR1-Bact

CTRL-LF > CTRL-RT; CTRL-LF

> SmR1-RT; CTRL-LF > SmR1-

Bact; CTRL-LF > SmR1-LF

Starch and CTRL-LF > CTRL-RT; CTRL-LF C00181 sucrose Monosaccharidea 5.60\* > SmR1-RT; CTRL-LF > SmR1-Bact; CTRL-LF > SmR1-LF metabolism CTRL-LF > CTRL-RT; CTRL-LF Diapolycopenedioat 17.87\* > SmR1-RT: CTRL-LF > SmR1е Bact; CTRL-LF > SmR1-LF CTRL-LF > CTRL-RT; CTRL-RT > SmR1-Bact; CTRL-LF > Miscellaneou Methylmalate 5.48\* SmR1-RT; CTRL-LF > SmR1s Bact; CTRL-LF > SmR1-LF;

C01546

5.47\*

**Agtuca** 

Furoic acida

<sup>\*</sup>P < 0.05

<sup>&</sup>lt;sup>a</sup> Metabolites assigned by in-house reference standard MS/MS performed under identical conditions.

Table S3. Pathways and metabolites in *Setaria viridis* colonized with SmR54 compared to the uninoculated plants. These metabolites were significant by ANOVA with a f-value range of 2 to 800. The samples that were analyzed were SmR54-RT, SmR54-LF, SmR54-Bact, CTRL-RT, and CTRL-LF.

Sample	Pathways	Metabolites	KEGG ID	f.value	Fisher's LSD
	Flavonoid	Methylpyranosyl glucoside <sup>a</sup>		12.12*	SmR54-RT > CTRL-RT; SmR54-RT > CTRL-LF; SmR54-RT > SmR54-Bact; SmR54-RT > SmR54-LF
	Biosynthesis	Hydroxyflavanone glucoside <sup>a</sup>	C16989	6.89*	SmR54-RT > CTRL-RT; SmR54-RT > CTRL-LF; SmR54-RT > SmR54-Bact; SmR54-RT > SmR54-LF
4-RT	Indole alkaloid	Norajmaline	C11810	43.14*	SmR54-RT > CTRL-RT; SmR54-RT > CTRL-LF; SmR54-RT > SmR54-Bact; SmR54-RT > SmR54-LF
SmR54-RT	biosynthesis	Ajmaline <sup>a</sup>	C06542	41.13*	SmR54-RT > CTRL-RT; SmR54-RT > CTRL-LF; SmR54-RT > SmR54-Bact; SmR54-RT > SmR54-LF
	Puromycin biosynthesis	Puromycin aminonucleoside	C01610	33.33*	SmR54-RT > CTRL-RT; SmR54-RT > CTRL-LF; SmR54-RT > SmR54-Bact; SmR54-RT > SmR54-LF
	Riboflavin metabolism	Lumichrome	C01727	4.89*	SmR54-RT > CTRL-RT; SmR54-RT > CTRL-LF; SmR54-RT > SmR54-Bact; SmR54-RT > SmR54-LF
	Amino acid metabolism	Oxoadipic acid <sup>a</sup>	C00322	3.55*	SmR54-LF > CTRL-RT; SmR54-LF > CTRL-LF; SmR54-LF > SmR54-RT; SmR54-LF > SmR54-Bact
	Chlorocyclohexa ne and chlorobenzene degradation	Glycolate	C00160	3.45*	SmR54-LF > CTRL-RT; SmR54-LF > SmR54-RT; SmR54-LF > SmR54-Bact
4-LF	Pentose Phosphate Pathway	Glucosaminate phosphate	C20589	4.41*	SmR54-LF > CTRL-RT; SmR54-LF > CTRL-LF; SmR54-LF > SmR54-RT; SmR54-LF > SmR54-Bact
SmR54-LF	Starch and sucrose	Heptose phosphate		9.03*	SmR54-LF > CTRL-RT; SmR54-LF > CTRL-LF; SmR54-LF > SmR54-RT; SmR54-LF > SmR54-Bact
	metabolism	Mannitol phosphate	C00644	3.49*	SmR54-LF > CTRL-RT; SmR54-LF > CTRL-LF; SmR54-LF > SmR54-RT; SmR54-LF > SmR54-Bact
	Miscellaneous	Benzoyloxyhydroxypr opyl glucopyranosiduronic acid <sup>a</sup>		5.82*	SmR54-LF > CTRL-RT; SmR54-LF > CTRL-LF; SmR54-LF > SmR54-RT; SmR54-LF > SmR54-Bact

					0 DE4 D 4 OTB: DT 0 DE45
		Sulfur dioxide	C09306	785.30*	SmR54-Bact > CTRL-RT; SmR54-Bact > CTRL-LF; SmR54-Bact > SmR54-RT; SmR54-Bact > SmR54-LF
	Amino acid metabolism	Glutathione <sup>a</sup>	C00051	30.30*	SmR54-Bact > CTRL-RT; SmR54-Bact > CTRL-LF; SmR54-Bact > SmR54-RT; SmR54-Bact > SmR54-LF
		Dihydroxybenzoate glucoside <sup>a</sup>	C00628	8.24*	SmR54-Bact > CTRL-RT; SmR54-Bact > CTRL-LF; SmR54-Bact > SmR54-RT; SmR54-Bact > SmR54-LF
	Calcium signaling pathway	Cyclic-ADP ribose <sup>a</sup>	C13050	32.61*	SmR54-Bact > CTRL-RT; SmR54-Bact > CTRL-LF; SmR54-Bact > SmR54-RT; SmR54-Bact > SmR54-LF
		Dihydroxyflavone glucoside <sup>a</sup>	C10216	43.62*	SmR54-Bact > CTRL-RT; SmR54-Bact > CTRL-LF; SmR54-Bact > SmR54-RT; SmR54-Bact > SmR54-LF
	Flavonoid Biosynthesis	Methyl glucoside <sup>a</sup>	C03619	17.05*	SmR54-Bact > CTRL-RT; SmR54-Bact > CTRL-LF; SmR54-Bact > SmR54-RT; SmR54-Bact > SmR54-LF
		Luteone	C10498	5.73*	SmR54-Bact > CTRL-RT; SmR54-Bact > CTRL-LF; SmR54-Bact > SmR54-RT; SmR54-Bact > SmR54-LF
-Bact		Adenine <sup>a</sup>	C00147	305.41*	SmR54-Bact > CTRL-RT; SmR54-Bact > CTRL-LF; SmR54-Bact > SmR54-RT; SmR54-Bact > SmR54-LF
SmR54-Bact		Adenosine diphosphate <sup>a</sup>	C00008	45.60*	SmR54-Bact > CTRL-RT; SmR54-Bact > CTRL-LF; SmR54-Bact > SmR54-RT; SmR54-Bact > SmR54-LF
		AMP <sup>a</sup>	C00020	39.17*	SmR54-Bact > CTRL-RT; SmR54-Bact > CTRL-LF; SmR54-Bact > SmR54-RT; SmR54-Bact > SmR54-LF
	Purine	Urate <sup>a</sup>	C00366	18.32*	SmR54-Bact > CTRL-RT; SmR54-Bact > CTRL-LF; SmR54-Bact > SmR54-RT; SmR54-Bact > SmR54-LF
	metabolism	UDP <sup>a</sup>	C00015	45.64*	SmR54-Bact > CTRL-RT; SmR54-Bact > CTRL-LF; SmR54-Bact > SmR54-RT; SmR54-Bact > SmR54-LF
		CMP <sup>a</sup>	C00055	11.56*	SmR54-Bact > CTRL-RT; SmR54-Bact > CTRL-LF; SmR54-Bact > SmR54-RT; SmR54-Bact > SmR54-LF
		Uridine <sup>a</sup>	C00299	8.30*	SmR54-Bact > CTRL-RT; SmR54-Bact > CTRL-LF; SmR54-Bact > SmR54-RT; SmR54-Bact > SmR54-LF
		CDP	C00112	5.53*	SmR54-Bact > CTRL-RT; SmR54-Bact > CTRL-LF; SmR54-Bact > SmR54-RT; SmR54-Bact > SmR54-LF
	Riboflavin metabolism	Amino (ribitylamino) uracil	C04732	16.86*	SmR54-Bact > CTRL-RT; SmR54-Bact > CTRL-LF; SmR54-Bact > SmR54-RT; SmR54-Bact > SmR54-LF

	Starch and sucrose metabolism	N-Acetyl-glucosamine phosphate <sup>a</sup>	C00357	60.14*	SmR54-Bact > CTRL-RT; SmR54-Bact > CTRL-LF; SmR54-Bact > SmR54-RT; SmR54-Bact > SmR54-LF
	Miscellaneous	Acetyl dihexose <sup>a</sup>		22.00*	SmR54-Bact > CTRL-RT; SmR54-Bact > CTRL-LF; SmR54-Bact > SmR54-RT; SmR54-Bact > SmR54-LF
	Aminobenzoate degradation	Dehydrodivanillate <sup>a</sup>	C18347	8.71*	CTRL-RT > CTRL-LF; CTRL-RT > SmR54-RT; CTRL-RT > SmR54-Bact; CTRL-RT > SmR54-LF; CTRL-LF > SmR54-Bact; SmR54-LF > SmR54-Bact; SmR54-LF > SmR54-Bact
	Butanoate	Maleate <sup>a</sup>	C01384	6.98*	CTRL-RT > SmR54-Bact;CTRL-LF > SmR54-RT;CTRL-LF > SmR54-Bact; SmR54-LF > SmR54-LF > SmR54-Bact
	metabolism	Malate <sup>a</sup>	C00497	5.29*	CTRL-RT > SmR54-Bact;CTRL-LF > SmR54-RT;CTRL-LF > SmR54-Bact; SmR54-LF > SmR54-RT; SmR54-LF > SmR54-Bact
		Luteolin glucuronide	C03515	9.67*	CTRL-RT > CTRL-LF; CTRL-RT > SmR54-RT; CTRL-RT > SmR54-Bact; SmR54-LF > CTRL-LF; SmR54-LF > SmR54-RT; SmR54-LF > SmR54-Bact
	Flavonoid Biosynthesis	Hydroxyjasmonic acid glucoside <sup>a</sup>	C08558	8.65*	CTRL-RT > CTRL-LF; CTRL-RT > SmR54-RT; CTRL-RT > SmR54-Bact; SmR54-LF > CTRL-LF; SmR54-LF > SmR54-RT; SmR54-LF > SmR54-Bact
CTRL-RT		Hydroxyflavone <sup>a</sup>	C11264	6.93*	CTRL-RT > CTRL-LF; CTRL-RT > SmR54-RT; CTRL-RT > SmR54-Bact; CTRL-RT > SmR54-LF
J		Coumesterola	C10205	5.40*	CTRL-RT > CTRL-LF; CTRL-RT > SmR54-Bact; CTRL-RT > SmR54-LF
		Quercetagetin glucoside <sup>a</sup>	C05623	4.70*	CTRL-RT > CTRL-LF; CTRL-RT > SmR54-RT; CTRL-RT > SmR54-Bact; CTRL-RT > SmR54-LF
		Acetyl-prenylphenol glucoside	C04608	4.64*	CTRL-RT > CTRL-LF; CTRL-RT > SmR54-RT; CTRL-RT > SmR54-Bact; CTRL-RT > SmR54-LF
		Leucocyanidin	C05906	3.40*	CTRL-RT > CTRL-LF; CTRL-RT > SmR54-RT; CTRL-RT > SmR54-Bact; CTRL-RT > SmR54-LF
		Sinapoylglucose <sup>a</sup>	C01175	7.26*	CTRL-RT > CTRL-LF; CTRL-RT > SmR54-RT; CTRL-RT > SmR54-Bact; CTRL-RT > SmR54-LF
	Phenylpropanoid biosynthesis	Pimpinellin <sup>a</sup>	C09285	6.84*	CTRL-RT > SmR54-RT; CTRL-RT > SmR54-Bact; CTRL-RT > SmR54- LF;CTRL-LF > SmR54-RT;CTRL-LF > SmR54-Bact
		Diphyllin	C10559	3.48*	CTRL-RT > CTRL-LF; CTRL-RT > SmR54-RT; CTRL-RT > SmR54-Bact;

		-			SmR54-LF > SmR54-RT; SmR54-LF > SmR54-Bact
	Riboflavin metabolism	Riboflavin cyclic phosphate	C16071	13.01*	CTRL-RT > CTRL-LF; CTRL-RT > SmR54-RT; SmR54-Bact > CTRL-RT; SmR54-Bact > CTRL-LF; SmR54-LF > CTRL-LF; SmR54-Bact > SmR54-RT; SmR54-LF > SmR54-LF > SmR54-LF
		Glucose phosphate <sup>a</sup>	C00103	11.36*	CTRL-RT > CTRL-LF; CTRL-RT > SmR54-RT; CTRL-RT > SmR54-Bact; CTRL-LF > SmR54-RT; SmR54-LF > CTRL-LF; SmR54-LF > SmR54-Bact
	Starch and sucrose metabolism	Sucrose <sup>a</sup>	C00089	9.60*	CTRL-RT > CTRL-LF; CTRL-RT > SmR54-RT; CTRL-RT > SmR54-Bact; SmR54-LF > CTRL-LF; SmR54-LF > SmR54-RT; SmR54-LF > SmR54-Bact
	•	Glucose <sup>a</sup>	C00031	5.14*	CTRL-RT > SmR54-RT; CTRL-RT > SmR54-Bact; CTRL-LF > SmR54-Bact; SmR54-LF > SmR54-LF > SmR54-Bact
	Terpenoid Biosynthesis	Methyl erythritol phosphate	C11434	4.47*	CTRL-RT > CTRL-LF; CTRL-RT > SmR54-RT; CTRL-RT > SmR54-Bact; CTRL-RT > SmR54-LF
		Shitimic acid <sup>a</sup>	C00493	7.31*	CTRL-LF > CTRL-RT; SmR54-LF > CTRL-RT;CTRL-LF > SmR54-RT;CTRL- LF > SmR54-Bact; SmR54-LF > SmR54-RT; SmR54-LF > SmR54-Bact
	Amino acid metabolism	Methylglyoxal	C00546	4.22*	CTRL-LF > SmR54-RT;CTRL-LF > SmR54-Bact; SmR54-LF > SmR54-RT; SmR54-LF > SmR54-Bact
		Phosphoglycerate	C00197	4.09*	CTRL-LF > CTRL-RT;CTRL-LF > SmR54-RT;CTRL-LF > SmR54-Bact;CTRL-LF > SmR54-LF
		Citrate <sup>a</sup>	C00158	3.68*	CTRL-LF > CTRL-RT;CTRL-LF > SmR54-RT;CTRL-LF > SmR54-Bact;CTRL-LF > SmR54-LF
CTRL-LF	Biosynthesis of plant hormones	Jasmonic acid <sup>a</sup>	C08491	3.57*	CTRL-LF > CTRL-RT;CTRL-LF > SmR54-RT;CTRL-LF > SmR54-Bact; SmR54-LF > SmR54-RT
	Glutathione metabolism	Ascorbic acid <sup>a</sup>	C00072	3.42*	CTRL-LF > CTRL-RT;CTRL-LF > SmR54-RT;CTRL-LF > SmR54-Bact
	Polycyclic aromatic hydrocarbon degradation	2-oxobut-3-enoate	C16149	8.10*	CTRL-LF > CTRL-RT;CTRL-LF > SmR54-RT;CTRL-LF > SmR54-Bact;CTRL-LF > SmR54-LF
	Purine metabolism	Oxoalate	C00209	7.16*	CTRL-LF > CTRL-RT; SmR54-LF > CTRL-RT;CTRL-LF > SmR54-RT;CTRL- LF > SmR54-Bact; SmR54-LF > SmR54-RT; SmR54-LF > SmR54-Bact
	metabolism	Glyoxylic acid	C00048	4.95*	CTRL-LF > CTRL-RT;CTRL-LF > SmR54-RT;CTRL-LF > SmR54-Bact;

				SmR54-LF > SmR54-RT; SmR54-LF > SmR54-Bact
	Pentose phosphate <sup>a</sup>		3.79*	CTRL-LF > SmR54-RT;CTRL-LF > SmR54-Bact; SmR54-LF > SmR54-RT; SmR54-LF > SmR54-Bact
Starch and sucrose metabolism	Monosaccharide <sup>a</sup>	C00181	7.58*	CTRL-LF > CTRL-RT;CTRL-LF > SmR54-RT;CTRL-LF > SmR54-Bact;CTRL-LF > SmR54-LF
	Diapolycopenedioate		12.83*	CTRL-LF > CTRL-RT;CTRL-LF > SmR54-RT;CTRL-LF > SmR54-Bact;CTRL-LF > SmR54-LF
Miscellaneous	Furoic acida	C01546	3.91*	CTRL-LF > CTRL-RT;CTRL-LF > SmR54-RT;CTRL-LF > SmR54-Bact
Miscenarieous	Methylmalate		3.74*	CTRL-LF > SmR54-RT;CTRL-LF > SmR54-Bact; SmR54-LF > SmR54-RT; SmR54-LF > SmR54-Bact
	Sequoyitol <sup>a</sup>	C03365	3.63*	CTRL-LF > CTRL-RT;CTRL-LF > SmR54-RT;CTRL-LF > SmR54-Bact

<sup>\*</sup>P < 0.05

<sup>&</sup>lt;sup>a</sup> Metabolites assigned by in-house reference standard MS/MS performed under identical conditions.

**Table S4.** Metabolites that were significantly present in *Setaria viridis* inoculated with SmR1 versus SmR54. These metabolites were significant by ANOVA with a f-value range of 3 to 212. The samples that were analyzed were SmR1-RT, SmR1-LF, SmR1-Bact, SmR54-RT, SmR54-LF, and SmR54-Bact.

Sample	Pathways	Metabolites	KEGG ID	f.value	Fisher's LSD
		Coumarate	C00811	4.09*	SmR1-RT > SmR1-Bact; SmR1-RT > SmR1-LF; SmR1-RT > SmR54-RT; SmR1-RT > SmR54-LF
	Amino acid metabolism	Phenylacetaldehyde	C00601	3.64*	SmR1-RT > SmR1-Bact; SmR1-RT > SmR1-LF; SmR1-RT > SmR54-RT; SmR1-RT > SmR54-LF
		Methylglutamate	C06034	3.10*	SmR1-RT > SmR1-Bact; SmR1-RT > SmR1-LF; SmR1-RT > SmR54-RT; SmR1-RT > SmR54-LF
	Biosynthesis of plant hormones	Jasmonic acid <sup>a</sup>	C08491	3.07*	SmR1-RT > SmR1-Bact; SmR1-RT > SmR54-Bact; SmR1-RT > SmR54-LF
	Butanoate metabolism Flavonoid biosynthesis	Maleate <sup>a</sup>	C01384	7.54**	SmR1-RT > SmR1-Bact; SmR1-RT > SmR1-LF; SmR1-RT > SmR54-Bact; SmR54-LF > SmR1-Bact; SmR54-LF > SmR1-LF; SmR54-LF > SmR54-RT; SmR54-LF > SmR54-Bact
SmR1-RT		Malate	C00497	4.81**	SmR1-RT > SmR1-Bact; SmR1-RT > SmR1-LF; SmR1-RT > SmR54-RT; SmR1-RT > SmR54-Bact; SmR54-LF > SmR1-Bact; SmR54-LF > SmR1-LF; SmR54-LF > SmR54-RT; SmR54-LF > SmR54-Bact
		Dihydroxy methoxyflavone glucoside <sup>a</sup>	C10381	9.72**	SmR1-RT > SmR1-Bact; SmR1-RT > SmR1-LF; SmR1-RT > SmR54-RT; SmR1-RT > SmR54-LF
		Coumesterola	C10205	8.64**	SmR1-RT > SmR1-Bact; SmR1-RT > SmR1-LF; SmR1-RT > SmR54-RT; SmR1- RT > SmR54-Bact; SmR1-RT > SmR54-LF; SmR54-RT > SmR1-Bact; SmR54-RT > SmR1-LF; SmR54-RT > SmR54-Bact; SmR54-RT > SmR54-LF
		Dihydroxy dimethoxyisoflavano ne		8.33**	SmR1-RT > SmR1-Bact; SmR1-RT > SmR1-LF; SmR1-RT > SmR54-RT; SmR1-RT > SmR54-Bact; SmR54-LF > SmR1-Bact; SmR54-LF > SmR1-LF; SmR54-RT; SmR54-LF > SmR54-RT; SmR54-LF > SmR54-Bact
		Dimethyltricetin		7.44**	SmR1-RT > SmR1-Bact; SmR1-RT > SmR1-LF; SmR1-RT > SmR54-RT; SmR1-RT > SmR54-Bact; SmR1-RT > SmR54-LF

	Dimethoxy-flavone	C10029	5.85**	SmR1-RT > SmR1-Bact; SmR1-RT > SmR1-LF; SmR1-RT > SmR54-RT; SmR1-RT > SmR54-Bact; SmR1-RT > SmR54-LF
	Glucoside malonate	C16222	5.80**	SmR1-RT > SmR1-Bact; SmR1-RT > SmR1-LF; SmR1-RT > SmR54-RT; SmR1-RT > SmR54-Bact; SmR1-RT > SmR54-LF
	Trihydroxyflavone <sup>a</sup>	C06563	4.72**	SmR1-RT > SmR1-Bact; SmR1-RT > SmR1-LF; SmR1-RT > SmR54-RT; SmR1-RT > SmR54-Bact; SmR1-RT > SmR54-LF
	Hydroxy methoxyflavone <sup>a</sup>		4.46**	SmR1-RT > SmR1-Bact; SmR1-RT > SmR1-LF; SmR1-RT > SmR54-RT; SmR1-RT > SmR54-Bact; SmR1-RT > SmR54-LF
	Dihydroxyisoflavone malonyl glucoside <sup>a</sup>	C16191	3.84*	SmR1-RT > SmR1-Bact; SmR1-RT > SmR1-LF; SmR1-RT > SmR54-RT; SmR1-RT > SmR54-Bact; SmR1-RT > SmR54-LF
	Quercetagetin glucoside <sup>a</sup>	C05623	3.81*	SmR1-RT > SmR1-Bact; SmR1-RT > SmR1-LF; SmR1-RT > SmR54-RT; SmR1-RT > SmR54-Bact; SmR1-RT > SmR54-LF
	Dihydroxy dimethoxyisoflavone glucoside		3.74*	SmR1-RT > SmR1-Bact; SmR1-RT > SmR1-LF; SmR1-RT > SmR54-RT; SmR1-RT > SmR54-Bact; SmR1-RT > SmR54-LF
	Tetramethoxyflavan one <sup>a</sup>	C14472	3.73*	SmR1-RT > SmR1-Bact; SmR1-RT > SmR1-LF; SmR1-RT > SmR54-RT; SmR1-RT > SmR54-Bact; SmR1-RT > SmR54-LF
	Hydroxyflavanone glucoside <sup>a</sup>	C16989	3.56*	SmR1-RT > SmR1-Bact; SmR1-RT > SmR1-LF; SmR1-RT > SmR54-Bact; SmR54-RT > SmR1-Bact; SmR54-RT > SmR1-LF; SmR54-RT > SmR54-LF; SmR54-RT > SmR54-LF
	Hydroxyflavone <sup>a</sup>	C11264	3.43*	SmR1-RT > SmR1-Bact; SmR1-RT > SmR1-LF; SmR1-RT > SmR54-RT; SmR1-RT > SmR54-Bact; SmR1-RT > SmR54-LF
	Hydroxybutyrate glucoside <sup>a</sup>		3.33*	SmR1-RT > SmR1-Bact; SmR1-RT > SmR1-LF; SmR1-RT > SmR54-RT; SmR1-RT > SmR54-Bact; SmR1-RT > SmR54-LF
	Acetyl-prenylphenol glucoside <sup>a</sup>	C04608	3.17*	SmR1-RT > SmR1-Bact; SmR1-RT > SmR1-LF; SmR1-RT > SmR54-RT; SmR1-RT > SmR54-Bact; SmR1-RT > SmR54-LF
Glyoxylate and dicarboxylate metabolism	Phosphoglycolic acid	C00988	4.25**	SmR1-RT > SmR1-Bact; SmR1-RT > SmR1-LF; SmR1-RT > SmR54-RT; SmR1-RT > SmR54-LF > SmR54-LF > SmR54-LF > SmR54-LF > SmR54-LF > SmR54-Bact; SmR54-Bact
Linolenic acid	Linoleic acid <sup>a</sup>	C01595	5.78**	SmR1-RT > SmR1-Bact; SmR1-RT > SmR1-LF; SmR1-RT > SmR54-RT; SmR1-RT > SmR54-Bact; SmR1-RT > SmR54-LF
metabolism	Epoxyoctadecadieno ic acid <sup>a</sup>	C16316	4.44**	SmR1-RT > SmR1-Bact; SmR1-RT > SmR1-LF; SmR1-RT > SmR54-Bact; SmR1-RT > SmR54-LF

		Epoxyoctadecenoic acid*	C08368	3.60*	SmR1-RT > SmR1-Bact; SmR1-RT > SmR1-LF; SmR1-RT > SmR54-RT; SmR1-RT > SmR54-Bact; SmR1-RT > SmR54-LF
	Phenylpropano id biosynthesis	Sinapoylglucosea	C01175	5.30**	SmR1-RT > SmR1-Bact; SmR1-RT > SmR1-LF; SmR1-RT > SmR54-RT; SmR1-RT > SmR54-Bact; SmR1-RT > SmR54-LF
	Purine	GMP <sup>a</sup>	C00144	4.94**	SmR1-RT > SmR1-Bact; SmR1-RT > SmR1-LF; SmR1-RT > SmR54-RT; SmR1- RT > SmR54-Bact; SmR54-LF > SmR1- Bact; SmR54-LF > SmR1-LF; SmR54-LF > SmR54-RT; SmR54-LF > SmR54-Bact
	metabolism	Glyoxylic acid	C00048	4.79**	SmR1-RT > SmR1-Bact; SmR1-RT > SmR54-RT; SmR1-RT > SmR54-Bact; SmR54-LF > SmR54-LF > SmR1-LF; SmR54-LF > SmR54-RT; SmR54-LF > SmR54-Bact
	Riboflavin metabolism	Lumichrome	C01727	3.94*	SmR1-RT > SmR1-Bact; SmR1-RT > SmR1-LF; SmR1-RT > SmR54-Bact; SmR1-RT > SmR54-RT > SmR1-RT > SmR54-RT > SmR1-Bact; SmR54-RT > SmR1-Bact; SmR54-RT > SmR54-RT > SmR54-RT > SmR54-RT > SmR54-LF
	Starch and sucrose	Glucose <sup>a</sup>	C00031	13.10**	SmR1-RT > SmR1-Bact; SmR1-RT > SmR54-RT; SmR1-RT > SmR54-Bact; SmR1-LF > SmR1-Bact; SmR54-LF > SmR1-Bact; SmR1-Bact; SmR1-Bact; SmR54-RT; SmR1-LF > SmR54-Bact; SmR54-Bact
	metabolism	Methylbutanoylapios ylhexose <sup>a</sup>	C11916	4.54**	SmR1-RT > SmR1-Bact; SmR1-RT > SmR1-LF; SmR1-RT > SmR54-RT; SmR1-RT > SmR54-Bact; SmR54-LF > SmR1-Bact; SmR54-LF > SmR54-RT
	Terpenoid biosynthesis	Farnesyl diphosphate	C00448	5.32**	SmR1-RT > SmR1-Bact; SmR1-RT > SmR1-LF; SmR1-RT > SmR54-RT; SmR1-RT > SmR54-Bact; SmR1-RT > SmR54-LF
	Zeatin biosynthesis	Zeatin <sup>a</sup>	C15545	4.92**	SmR1-RT > SmR1-Bact; SmR1-RT > SmR1-LF; SmR1-RT > SmR54-RT; SmR1-RT > SmR54-Bact; SmR1-RT > SmR54-LF
	Miscellaneous	Sulfolactaldehyde	C20798	15.60**	SmR1-RT > SmR1-Bact; SmR1-RT > SmR1-LF; SmR1-RT > SmR54-RT; SmR1- RT > SmR54-Bact; SmR1-RT > SmR54-LF; SmR54-RT > SmR1-Bact; SmR54-RT > SmR1-LF; SmR54-RT > SmR54-Bact; SmR54-RT > SmR54-LF
	Amino acid metabolism	Citrate <sup>a</sup>	C00158	6.26**	SmR1-LF > SmR1-RT; SmR1-LF > SmR1- Bact; SmR1-LF > SmR54-RT; SmR1-LF > SmR54-Bact; SmR1-LF > SmR54-LF
SmR1-LF	Aminobenzoat e degradation	Dehydrodivanillate <sup>a</sup>	C18347	6.80**	SmR1-LF > SmR1-RT; SmR54-LF > SmR1-RT; SmR1-LF > SmR1-Bact; SmR54-LF > SmR1-Bact; SmR1-LF > SmR54-RT; SmR1-LF > SmR54-Bact; SmR54-LF > SmR54-RT; SmR54-LF > SmR54-Bact
	I				

					0 8415: 0 8487 0 8415: 0 84
	Butanoate metabolism	Butanediol	C03044	3.20*	SmR1-LF > SmR1-RT; SmR1-LF > SmR1- Bact; SmR1-LF > SmR54-RT; SmR1-LF > SmR54-Bact; SmR1-LF > SmR54-LF
	Glutathione metabolism	Ascorbic acid <sup>a</sup>	C00072	11.64**	SmR1-LF > SmR1-RT; SmR54-LF > SmR1-RT; SmR1-LF > SmR1-Bact; SmR54-LF > SmR1-Bact; SmR1-LF > SmR54-RT; SmR1-LF > SmR54-Bact; SmR54-LF > SmR1-LF; SmR54-LF > SmR54-RT; SmR54-LF > SmR54-Bact
	Glyoxylate and dicarboxylate metabolism	Mesaconate <sup>a</sup>	C01732	3.15*	SmR1-LF > SmR1-Bact; SmR54-LF > SmR1-Bact; SmR1-LF > SmR54-Bact; SmR54-LF > SmR54-RT; SmR54-LF > SmR54-Bact
	Phenylpropano id biosynthesis	Diphyllin	C10559	6.82**	SmR1-LF > SmR1-RT; SmR1-LF > SmR1-Bact; SmR54-LF > SmR1-Bact; SmR1-LF > SmR54-RT; SmR1-LF > SmR54-Bact; SmR54-LF > SmR54-RT; SmR54-LF > SmR54-Bact
	Miscellaneous	Methylmalate		4.50**	SmR1-LF > SmR1-Bact; SmR54-LF > SmR1-Bact; SmR1-LF > SmR54-RT; SmR1-LF > SmR54-Bact; SmR54-LF > SmR54-RT; SmR54-RT; SmR54-LF > SmR54-Bact
	Amino acid metabolism	Sulfur dioxide	C09306	212.51* *	SmR1-Bact > SmR1-RT; SmR54-Bact > SmR1-RT; SmR1-Bact > SmR1-LF; SmR1- Bact > SmR54-RT; SmR54-Bact > SmR1- Bact; SmR1-Bact > SmR54-LF; SmR54- Bact > SmR1-LF; SmR54-Bact > SmR54- RT; SmR54-Bact > SmR54-LF
	metabolism	Dihydroxybenzoate glucoside <sup>a</sup>	C00628	6.69**	SmR1-Bact > SmR1-RT; SmR54-Bact > SmR1-RT; SmR1-Bact > SmR1-LF; SmR1-Bact > SmR54-RT; SmR1-Bact > SmR54-LF; SmR54-Bact > SmR54-Bact > SmR54-Bact > SmR54-RT; SmR54-Bact > SmR54-LF
1-Bact	Calcium signaling pathway	Cyclic-ADP ribose <sup>a</sup>	C13050	55.76**	SmR1-Bact > SmR1-RT; SmR54-Bact > SmR1-RT; SmR1-Bact > SmR1-LF; SmR1-Bact > SmR54-Bact > SmR54-Bact; SmR1-Bact > SmR54-Bact; SmR1-Bact > SmR54-Bact > SmR1-LF; SmR54-Bact > SmR1-LF; SmR54-Bact > SmR54-LF; SmR54-Bact > SmR54-Bact > SmR54-Bact > SmR54-Bact > SmR54-Bact > SmR54-Bact > SmR54-LF
SmR1-B	Flavonoid	Dihydroxyflavone glucoside <sup>a</sup>	C10216	31.26**	SmR1-Bact > SmR1-RT; SmR54-Bact > SmR1-RT; SmR1-Bact > SmR1-LF; SmR1-Bact > SmR54-RT; SmR1-Bact > SmR54-LF; SmR54-Bact > SmR54-Bact > SmR54-RT; SmR54-Bact > SmR54-LF
	biosynthesis	Luteolin glucuronide	C03515	3.58*	SmR1-Bact > SmR1-RT; SmR1-Bact > SmR1-LF; SmR1-Bact > SmR54-RT; SmR1-Bact > SmR54-LF > SmR1-LF; SmR54-LF > SmR54-LF; SmR54-LF > SmR5
	Purine metabolism	Fructose biphosphate <sup>a</sup>	C06193	84.41**	SmR1-Bact > SmR1-RT; SmR54-Bact > SmR1-RT; SmR1-Bact > SmR1-LF; SmR1- Bact > SmR54-RT; SmR54-Bact > SmR1- Bact; SmR1-Bact > SmR54-LF; SmR54- Bact > SmR1-LF; SmR54-Bact > SmR54- RT; SmR54-Bact > SmR54-LF

SmR1-Bact > SmR1-RT; SmR54-Bact > SmR1-RT; SmR1-Bact > SmR1-LF; SmR1- Adenine*  C00147 77.10**  Bact > SmR54-RT; SmR1-Bact > SmR54- Bact > SmR54-RT; SmR1-Bact > SmR54- C00147 77.10**	
Bact; SmR1-Bact > SmR54-LF; SmR54- Bact > SmR1-LF; SmR54-Bact > SmR54- RT; SmR54-Bact > SmR54-LF	
SmR1-Bact > SmR1-RT; SmR54-Bact > SmR1-Bact > SmR1-RT; SmR1-LF; SmR1- SmR1-Bact > SmR1-Bact > SmR1-LF; SmR1-Bact > SmR54-LF; SmR54- Bact; SmR1-Bact > SmR54-LF; SmR54- Bact > SmR1-LF; SmR54-Bact > SmR54-LF; SmR54-LF; SmR54-LF; SmR54-LF	
SmR1-Bact > SmR1-RT; SmR54-Bact > SmR1-RT; SmR54-Bact > SmR1-RT; SmR1-Bact > SmR1-LF; SmR1-Bact > SmR1-LF; SmR1-Bact > SmR1-Bact > SmR54-Bact > SmR54-Bact > SmR54-LF; SmR54-Bact > SmR54-LF; SmR54-Bact > SmR54-LF; SmR54-Bact > SmR54-LF; SmR54-LF	
SmR1-Bact > SmR1-RT; SmR54-Bact > SmR1-RT; SmR54-Bact > SmR1-RT; SmR1-Bact > SmR1-RT; SmR1-Bact > SmR1-RT; SmR1-Bact > SmR54-RT; SmR1-Bact > SmR54-RT; SmR54-Bact > SmR54-LF; SmR54-Bact > SmR1-LF; SmR54-Bact > SmR54-LF; SmR54-Bact > SmR54-LF; SmR54-Bact > SmR54-LF	
SmR1-Bact > SmR1-RT; SmR54-Bact > SmR1-RT; SmR54-Bact > SmR1-RT; SmR1-Bact > SmR1-LF; SmR1-LF; SmR1-Bact > SmR54-RT; SmR1-Bact > SmR54-LF; SmR54-Bact; SmR1-Bact > SmR54-LF; SmR54-Bact > SmR54-Bact > SmR54-Bact > SmR54-LF; SmR54-LF	
Guanosine C06193 17.27** SmR1-Bact > SmR1-RT; SmR1-Bact > SmR54-RT; SmR1-Bact > SmR54-Bact; SmR1-Bact > SmR54-LF	
SmR1-Bact > SmR1-RT; SmR54-Bact > SmR1-RT; SmR54-Bact > SmR1-RT; SmR1-Bact > SmR1-LF; SmR1-Bact > SmR1-RT; SmR1-Bact > SmR1-LF; SmR1-Bact > SmR54-Bact > SmR54-	
SmR1-Bact > SmR1-RT; SmR1-Bact >   Guanosine   C00387   9.53**   SmR1-LF; SmR1-Bact > SmR54-RT; SmR1-Bact > SmR54-Bact; SmR1-Bact > SmR54-LF	
SmR1-Bact > SmR1-RT; SmR54-Bact > SmR1-RT; SmR1-LF; SmR1-LF; SmR1-LF; SmR1-LF; SmR1-Bact > SmR1-RT; SmR1-Bact > SmR1-LF; SmR1-Bact > SmR54-RT; SmR1-Bact > SmR54-LF; SmR54-Bact; SmR1-Bact > SmR54-LF; SmR54-Bact > SmR54-RT	
Pyrimidine metabolism         SmR1-Bact > SmR1-RT; SmR54-Bact > SmR1-LF; SmR1-Bact > SmR1-RT; SmR1-Bact > SmR1-LF; SmR1-Bact > SmR1-LF; SmR54-Bact > SmR1-LF; SmR54-Bact > SmR54-LF; SmR54-Bact > SmR54-LF; SmR54-Bact > SmR1-LF; SmR54-Bact > SmR54-LF; SmR54-Bact > SmR54-LF	
CMP <sup>a</sup> C00055 12.45** SmR1-Bact > SmR1-RT; SmR54-Bact > SmR1-RT; SmR1-LF; SmR1-LF; SmR1-RT; SmR1-Bact > SmR1-RT; SmR1-Bact > SmR1-RT; SmR1	

Bact   SmR4HRT   SmR1-Bact   SmR4HRT						
Pyruvate metabolism			СМР	C00941	11.05**	Bact; SmR1-Bact > SmR54-LF; SmR54- Bact > SmR1-LF; SmR54-Bact > SmR54- RT; SmR54-Bact > SmR54-LF SmR1-Bact > SmR1-RT; SmR1-Bact > SmR1-LF; SmR1-Bact > SmR54-RT; SmR1-Bact > SmR54-Bact; SmR1-Bact >
Riboflavin metabolism			Lactoylglutathione	C03451	5.64**	SmR1-Bact > SmR1-RT; SmR1-Bact > SmR1-LF; SmR1-Bact > SmR54-RT; SmR1-Bact > SmR54-Bact >
Acetylneuraminic acid			• •	C04732	30.34**	SmR1-RT; SmR1-Bact > SmR1-LF; SmR1- Bact > SmR54-RT; SmR1-Bact > SmR54- Bact; SmR1-Bact > SmR54-LF; SmR54- Bact > SmR1-LF; SmR54-Bact > SmR54-
Starch and sucrose metabolism				C00270	52.02**	SmR1-RT; SmR1-Bact > SmR1-LF; SmR1- Bact > SmR54-RT; SmR1-Bact > SmR54- LF; SmR54-Bact > SmR1-LF; SmR54-Bact
Acetyl dihexose		sucrose		C00357	49.45**	SmR1-RT; SmR1-Bact > SmR1-LF; SmR1- Bact > SmR54-RT; SmR54-Bact > SmR1- Bact; SmR1-Bact > SmR54-LF; SmR54- Bact > SmR1-LF; SmR54-Bact > SmR54-
Name			dTDP-hexose	C00842	4.98**	SmR1-LF; SmR1-Bact > SmR54-RT; SmR1-Bact > SmR54-Bact; SmR1-Bact >
Riboflavin cyclic phosphate			Isopentenyl-ADP	C16426	3.34*	SmR1-LF; SmR1-Bact > SmR54-RT; SmR1-Bact > SmR54-Bact; SmR1-Bact >
Acetyl dihexose <sup>a</sup> Acetyl dihexose <sup>a</sup> 25.54**  SmR1-RT; SmR1-Bact > SmR54-LF; SmR1-Bact > SmR54-LF; SmR54-Bact > SmR54-RT; SmR54-Bact > SmR54-RT; SmR54-Bact > SmR54-RT > SmR54-RT > SmR54-RT > SmR1-Bact; SmR54-RT > SmR1-Bact; SmR54-RT > SmR1-Bact; SmR54-RT > SmR5		Miscellaneous	•	C16071	59.17**	SmR1-RT; SmR1-Bact > SmR1-LF; SmR1- Bact > SmR54-RT; SmR1-Bact > SmR54- Bact; SmR1-Bact > SmR54-LF; SmR54- Bact > SmR1-LF; SmR54-Bact > SmR54-
Methylpyranosyl glucosidea   9.81**   SmR1-Bact; SmR54-RT > SmR1-LF; SmR54-BT > SmR1-Bact; SmR54-BT > SmR1-Bact; SmR54-			Acetyl dihexose <sup>a</sup>		25.54**	SmR1-RT; SmR1-Bact > SmR1-LF; SmR1- Bact > SmR54-RT; SmR1-Bact > SmR54- LF; SmR54-Bact > SmR1-LF; SmR54-Bact
,	(54-RT				9.81**	SmR1-Bact; SmR54-RT > SmR1-LF; SmR54-RT > SmR54-Bact; SmR54-RT >
	SmR	biosynthesis	Methyl glucoside <sup>a</sup>	C03619	3.08*	SmR1-Bact; SmR54-RT > SmR1-LF;

	Indole alkaloid	Norajmaline	C11810	29.09**	SmR54-RT > SmR1-RT; SmR1-RT > SmR1-Bact; SmR1-RT > SmR1-LF; SmR1- RT > SmR54-Bact; SmR1-RT > SmR54-LF; SmR54-RT > SmR1-Bact; SmR54-RT > SmR1-LF; SmR54-RT > SmR54-Bact; SmR54-RT > SmR54-LF
	biosynthesis	Ajmalineª	C06542	24.11**	SmR54-RT > SmR1-RT; SmR1-RT > SmR1-Bact; SmR1-RT > SmR1-LF; SmR1- RT > SmR54-Bact; SmR1-RT > SmR54-LF; SmR54-RT > SmR1-Bact; SmR54-RT > SmR1-LF; SmR54-RT > SmR54-Bact; SmR54-RT > SmR54-LF
	Puromycin biosynthesis	Puromycin aminonucleoside	C01610	23.64**	SmR54-RT > SmR1-RT; SmR1-RT > SmR1-Bact; SmR1-RT > SmR1-LF; SmR1- RT > SmR54-Bact; SmR1-RT > SmR54-LF; SmR54-RT > SmR1-Bact; SmR54-RT > SmR1-LF; SmR54-RT > SmR54-Bact; SmR54-RT > SmR54-LF
		Shitimic acid <sup>a</sup>	C00493	7.81**	SmR54-LF > SmR1-RT; SmR1-LF > SmR1-Bact; SmR54-LF > SmR1-Bact; SmR1-LF > SmR54-LF > SmR1-LF; SmR54-LF > SmR54-LF; SmR54-LF > SmR54-Bact
	Amino acid	Glutathione <sup>a</sup>	C00051	4.59**	SmR54-LF > SmR1-RT; SmR54-LF > SmR1-Bact; SmR54-LF > SmR1-LF; SmR54-LF > SmR54-LF > SmR54-Bact
	metabolism	Methylglyoxal	C00546	4.47**	SmR54-LF > SmR1-RT; SmR54-LF > SmR1-Bact; SmR54-LF > SmR1-LF; SmR54-LF > SmR54-LF > SmR54-Bact
		Sulfolactate/phosph olactate <sup>a</sup>	C11537	3.25*	SmR54-LF > SmR1-RT; SmR54-LF > SmR1-Bact; SmR54-LF > SmR1-LF; SmR54-LF > SmR54-LF > SmR54-LF > SmR54-Bact
SmR54-LF	Chlorocyclohe xane and chlorobenzene degradation	Glycolate	C00160	4.78**	SmR54-LF > SmR1-RT; SmR54-LF > SmR1-Bact; SmR54-LF > SmR1-LF; SmR54-LF > SmR54-LF > SmR54-Bact
		Kaempferol rhamnoside glucoside	C21854	10.94**	SmR54-LF > SmR1-RT; SmR54-LF > SmR1-Bact; SmR54-LF > SmR1-LF; SmR54-LF > SmR54-LF > SmR54-Bact
	Flavonoid biosynthesis	Pentahydroxy methoxyflavone	C04527	5.18**	SmR54-LF > SmR1-RT; SmR54-LF > SmR1-Bact; SmR54-LF > SmR1-LF; SmR54-LF > SmR54-LF > SmR54-Bact
		Hydroxyjasmonic acid glucoside <sup>a</sup>	C08558	4.65**	SmR54-LF > SmR1-RT; SmR54-LF > SmR1-Bact; SmR54-LF > SmR1-LF; SmR54-LF > SmR54-LF > SmR54-Bact
	Pentose phosphate pathway	Glucosaminate phosphate	C20589	4.70**	SmR54-LF > SmR1-RT; SmR54-LF > SmR1-Bact; SmR54-LF > SmR1-LF;

Chavicol   C16930   5.91**   SmR54-LF > SmR1-RT; SmR54-LF > SmR1-RT; SmR54-LF > SmR54-Bact   SmR54-Bact   SmR54-Bact   SmR54-LF > SmR54-Bact   SmR54-Bact   SmR54-Bact   SmR54-LF > SmR54-LF > SmR54-LF > SmR54-LF > SmR54-LF > SmR54-LF > SmR54-Bact   SmR54-LF >						SmR54-LF > SmR54-RT; SmR54-LF >
Chavicol   C16930   5.91**   SmR1-Bact; SmR54-LF > SmR1-LF; SmR54-LF > SmR5						·
Pimpinellina			Chavicol	C16930	5.91**	SmR1-Bact; SmR54-LF > SmR1-LF; SmR54-LF > SmR54-RT; SmR54-LF >
Purine metabolism		iu biosyntiiesis	Pimpinellin <sup>a</sup>	C09285	4.20*	SmR1-LF; SmR54-LF > SmR54-RT;
Pentose phosphatea   5.31**   Sint34-LF > SmR1-Bact; SmR54-LF > SmR1-Bact; SmR54-LF > SmR54-Bact   SmR54-LF >			Oxoalate	C00209	5.90**	SmR1-Bact; SmR54-LF > SmR1-LF; SmR54-LF > SmR54-RT; SmR54-LF >
Sucrosea		metabolism	Pentose phosphate <sup>a</sup>		5.31**	SmR1-Bact; SmR54-LF > SmR1-Bact; SmR1-LF > SmR54-Bact; SmR54-LF >
Statch and sucrose metabolism			Sucrose <sup>a</sup>	C00089	8.66**	SmR1-Bact; SmR54-LF > SmR1-LF; SmR54-LF > SmR54-RT; SmR54-LF >
Trisaccharide  3.83*  SmR1-Bact; SmR54-LF > SmR1-LF; SmR54-LF > SmR1-LF; SmR54-LF > SmR54-LF > SmR54-LF > SmR54-LF > SmR54-Bact  Terpenoid Biosynthesis  Methyl erythritol phosphate  C11434  6.95**  SmR54-LF > SmR1-RT; SmR54-LF > SmR1-LF; SmR54-LF > SmR54-LF > SmR54-LF > SmR54-LF > SmR54-LF > SmR54-Bact  Benzoyloxyhydroxyp ropyl glucopyranosiduroni  6.64**  SmR54-LF > SmR1-RT; SmR54-LF > SmR1-RT; SmR54-LF > SmR1-RT; SmR54-LF >		sucrose	Glucose phosphatea	C00103	8.42**	SmR1-Bact; SmR54-LF > SmR1-LF; SmR54-LF > SmR54-RT; SmR54-LF >
Terpenoid Biosynthesis  Methyl erythritol phosphate  C11434  6.95**  SmR1-Bact; SmR54-LF > SmR1-LF; SmR54-LF >			Trisaccharide		3.83*	SmR1-Bact; SmR54-LF > SmR1-LF; SmR54-LF > SmR54-RT; SmR54-LF >
ropyl $6.64^{**}$ SmR1-Bact; SmR54-LF > SmR1-LF; SmR54-LF > SmR54-LF > SmR54-LF >				C11434	6.95**	SmR1-Bact; SmR54-LF > SmR1-LF; SmR54-LF > SmR54-RT; SmR54-LF >
			ropyl		6.64**	SmR1-Bact; SmR54-LF > SmR1-LF; SmR54-LF > SmR54-RT; SmR54-LF >
Miscellaneous Furoic acid <sup>a</sup> C01546 3.53* SmR54-LF > SmR1-RT; SmR54-LF > SmR1-Bact; SmR54-LF > SmR54-LF > SmR54-LF > SmR54-LF > SmR54-LF > SmR54-Bact		Miscellaneous	Furoic acid <sup>a</sup>	C01546	3.53*	SmR1-Bact; SmR54-LF > SmR1-LF; SmR54-LF > SmR54-RT; SmR54-LF >
SmR54-LF > SmR1-RT; SmR54-LF >  Metaphosphoric acid C02466 3.08* SmR1-Bact; SmR54-LF > SmR1-LF; SmR54-LF > SmR54-LF > SmR54-LF > SmR54-Bact			Metaphosphoric acid	C02466	3.08*	SmR1-Bact; SmR54-LF > SmR1-LF; SmR54-LF > SmR54-RT; SmR54-LF >
Flavonoid biosynthesis  Luteone  C10498  C10498  End on the biosynthesis  Flavonoid biosynthesis  Flavonoid biosynthesis  C10498  C104	Ko4-bact		Luteone	C10498	5.65**	SmR1-Bact; SmR54-Bact > SmR1-LF; SmR54-Bact > SmR54-RT; SmR54-Bact >
Pyrimidine Uridine <sup>a</sup> C00299 7.95** SmR54-Bact > SmR1-RT; SmR54-Bact > SmR1-Bact; SmR54-Bact > SmR1-LF;	Ē	Pyrimidine	Uridine <sup>a</sup>	C00299	7.95**	

Agtuca

metabolism				SmR54-Bact > SmR54-RT; SmR54-Bact > SmR54-LF
	CDP	C00112	5.19**	SmR54-Bact > SmR1-RT; SmR54-Bact > SmR1-Bact; SmR54-Bact > SmR1-LF; SmR54-Bact > SmR54-Bact > SmR54-LF

MPMI

<sup>&</sup>lt;sup>a</sup> Metabolites assigned by in-house reference standard MS/MS performed under identical conditions.



<sup>\*</sup>P < 0.05 and \*\*P < 0.005